THE JOURNAL OF BIOLOGICAL CHEMISTRY VOL. 287, NO. 19, pp. 15345–15364, May 4, 2012

α-Synuclein in Central Nervous System and from Erythrocytes, Mammalian Cells, and *Escherichia coli* Exists Predominantly as Disordered Monomer*[S]

Received for publication, November 1, 2011, and in revised form, January 21, 2012 Published, JBC Papers in Press, February 7, 2012, DOI 10.1074/jbc.M111.318949

Bruno Fauvet[‡], Martial K. Mbefo[‡], Mohamed-Bilal Fares[‡], Carole Desobry[‡], Sarah Michael[§], Mustafa T. Ardah[¶], Elpida Tsika[‖], Philippe Coune[**], Michel Prudent[‡‡], Niels Lion[‡‡], David Eliezer[§§], Darren J. Moore[‖], Bernard Schneider[**], Patrick Aebischer[**], Omar M. El-Agnaf[¶], Eliezer Masliah[§], and Hilal A. Lashuel[‡1]

*From the [‡]Laboratory of Molecular and Chemical Biology of Neurodegeneration, Brain Mind Institute, Station 19, School of Life Sciences, Ecole Polytechnique Fédérale de Lausanne, CH-1015 Lausanne, Switzerland, the [§]Department of Neurosciences, School of Medicine, University of California at San Diego, La Jolla, California 92093, the [¶]Department of Biochemistry, Faculty of Medicine and Health Sciences, United Arab Emirates University, Al Ain 15551, United Arab Emirates, the [‖]Laboratory of Molecular Neurodegenerative Research, **Neurodegenerative Disease Laboratory, Ecole Polytechnique Fédérale de Lausanne, CH-1015 Lausanne, Switzerland, the [‡‡]Service Régional Vaudois de Transfusion Sanguine, Route de la Corniche 2, 1066 Epalinges, Switzerland, and the [§§]Department of Biochemistry and Program in Structural Biology, Weill Cornell Medical College, New York, New York 10065*

Background: The oligomeric state of α-syn *in vivo* remains unknown.
Results: α-syn in the CNS and produced by erythrocytes, mammalian cells, and *Escherichia coli* exists predominantly as a disordered monomer.
Conclusion: Native α-syn from various sources behaves as unstructured and monomeric.
Significance: Stabilizing monomeric α-syn, lowering its levels, and/or inhibiting its fibrillization remain viable therapeutic strategies for Parkinson disease.

Since the discovery and isolation of α-synuclein (α-syn) from human brains, it has been widely accepted that it exists as an intrinsically disordered monomeric protein. Two recent studies suggested that α-syn produced in *Escherichia coli* or isolated from mammalian cells and red blood cells exists predominantly as a tetramer that is rich in α-helical structure (Bartels, T., Choi, J. G., and Selkoe, D. J. (2011) *Nature* 477, 107–110; Wang, W., Perovic, I., Chittuluru, J., Kaganovich, A., Nguyen, L. T. T., Liao, J., Auclair, J. R., Johnson, D., Landeru, A., Simorellis, A. K., Ju, S., Cookson, M. R., Asturias, F. J., Agar, J. N., Webb, B. N., Kang, C., Ringe, D., Petsko, G. A., Pochapsky, T. C., and Hoang, Q. Q. (2011) *Proc. Natl. Acad. Sci.* 108, 17797–17802). However, it remains unknown whether or not this putative tetramer is the main physiological form of α-syn in the brain. In this study, we investigated the oligomeric state of α-syn in mouse, rat, and human brains. To assess the conformational and oligomeric state of native α-syn in complex mixtures, we generated α-syn standards of known quaternary structure and conformational properties and compared the behavior of endogenously expressed α-syn to these standards using native and denaturing gel electrophoresis techniques, size-exclusion chromatography, and an oligomer-specific ELISA. Our findings demonstrate that both human and rodent α-syn expressed in the central nervous system exist predominantly as an unfolded monomer. Similar results were observed when human α-syn was expressed in mouse and rat brains as well as mammalian cell lines (HEK293, HeLa, and SH-SY5Y). Furthermore, we show that α-syn expressed in *E. coli* and purified under denaturing or nondenaturing conditions, whether as a free protein or as a fusion construct with GST, is monomeric and adopts a disordered conformation after GST removal. These results do not rule out the possibility that α-syn becomes structured upon interaction with other proteins and/or biological membranes.

α-Synuclein (α-syn)[2] is a 140-residue protein that is highly expressed in the central nervous system and is the major constituent of Lewy bodies (LBs), the intracellular protein inclusions commonly found in post-mortem human brains of Parkinson disease patients (3, 4). Although the precise mechanism by which LB formation contributes to neurotoxicity and the loss of dopaminergic neurons are not yet completely understood, strong circumstantial evidence from various sources (genetics, pathology, cell culture, and transgenic models) sup-

* This work was supported, in whole or in part, by National Institutes of Health Grant AG019391 from NIA (to D. E.). This work was also supported by grants from the Michael J. Fox Foundation for Parkinson Research (to H. A. L., D. J. M., and O. M. E.), the Swiss National Science Foundation Grants 31003AB_135696DE (to P. C., B. S., and P. A.) and 31003A_120653 (to H. A. L., B. F., and M.-B. F.), the United Arab Emirates University (to M. T. A. and O. M. E.), Swiss Federal Institute of Technology, Lausanne (to H. A. L., D. J. M., P. C., B. S., and P. A.), an ERC starting grant (to B. F., C. A. D., and H. A. L.), and a Merck Serono grant (to M.-B. F., and H. A. L.). This work was partially funded by as grant from Merck Serono.
[S] This article contains supplemental Figs. S1–S7.
[1] To whom correspondence should be addressed. Tel.: 41 21 693 96 91; Fax: 41 21 693 17 80; E-mail: hilal.lashuel@epfl.ch.

[2] The abbreviations used are: α-syn, α-synuclein; LB, Lewy body; DLB, dementia with LB; AD, Alzheimer disease; CV, column volume; EC, erythrocyte concentrate; SEC, size-exclusion chromatography; BisTris, 2-[bis(2-hydroxyethyl)amino]-2-(hydroxymethyl)propane-1,3-diol; TG, transgenic mice; POPG, phosphatidylglycerol; AAV, adeno-associated virus; SNpc, substantia nigra pars compacta; HIC, hydrophobic interaction chromatography; CN-PAGE, Clear Native-PAGE; BS^3, bis(sulfosuccinimidyl) suberate.

ports a direct link between the propensity of α-syn to undergo oligomerization and its deleterious effects in the brain (reviewed in Ref. 5).

Since its discovery and isolation from human brains, it has been widely accepted that α-syn exists as an intrinsically disordered monomeric protein (6, 7). Increased expression (resulting from genomic multiplication of the SNCA locus (8, 9)), missense mutations (A30P, A53T, and E46K (10–12)), oxidative stress (13–16), or increased exposure to heavy metal ions (17, 18) promotes the misfolding and self-assembly of α-syn into toxic β-sheet-rich high molecular weight oligomers and amyloid fibrils. Therefore, current efforts aimed at targeting α-syn for the treatment of Parkinson disease and related disorders are focused on preventing its misfolding and aggregation by the following: 1) reducing its expression, 2) promoting its clearance, and 3) stabilizing the monomeric form of the protein and/or blocking its assembly into toxic oligomers or fibrils.

A recent study by Bartels *et al.* (1) suggests that in red blood cells (RBCs) and mammalian cell lines, α-syn exists as a stable tetramer that is rich in α-helical structure and is resistant to amyloid formation. A subsequent study by Wang *et al.* (2) suggested that α-syn expressed in *Escherichia coli* exists as dynamic tetramer that is rich in α-helical structure. However, it remains unknown whether or not this putative tetramer is the main physiological form of α-syn in the brain. In this study, we investigated the oligomeric state of α-syn in mouse, rat, and human brains. To assess the conformational and oligomeric state of native α-syn in complex mixtures, we employed native and denaturing gel electrophoresis techniques, size-exclusion chromatography, and oligomer-specific ELISA. Our findings demonstrate that endogenous and overexpressed α-syn in human, mouse, and rat brains exists predominantly in a monomeric state and co-migrates with the unfolded recombinant monomeric α-syn in native gels and gel-filtration columns. Similarly, endogenous or overexpressed human α-syn expressed in mammalian cell lines (HEK293, HeLa, and SH-SY5Y) behaved similarly to unfolded monomeric α-syn in all assays performed in this study. These results and the report by Wang *et al.* (2) prompted us to reinvestigate the oligomeric state of recombinant α-syn produced in *E. coli*. Our studies confirmed previous findings by multiple groups demonstrating that α-syn expressed in *E. coli* and purified under denaturing or nondenaturing conditions, whether expressed alone or as a fusion with GST, is monomeric and adopts a predominantly disordered conformation (6, 19, 20). The strength of the work presented here comes from the convergence of our results, performed independently by a total of seven independent research groups using multiple methods.

EXPERIMENTAL PROCEDURES

Plasmids—The pT7-7 plasmids were used for the expression of recombinant human α-syn in *E. coli*. The following two plasmids used for the preparation of the GST-α-syn fusion proteins pGEX-2TK (in the Lashuel group) and pGEX-4T1 (in the El-Agnaf group) were kind gifts from the laboratories of Dr. Julia George (University of Illinois, Urbana-Champaign) and Dr. Hyangshuk Rhim (The Catholic University College of Medicine, Seoul, Korea), respectively. For the production of AAVs, human WT α-syn, cDNA (GenBank™ accession number NM_000345) was inserted in the pAAV-PGK-MCS backbone modified from the pAAV-CMV-MCS plasmid (Stratagene, La Jolla, CA) using standard cloning procedures. All constructs were confirmed by DNA sequencing (Microsynth, Switzerland) using the standard primers provided by the supplier.

Expression and Purification of Recombinant WT Human α-syn Monomers and A140C Disulphide-linked Dimers—BL21(DE3) cells transformed with a pT7-7 plasmid encoding WT human α-syn were freshly grown on an ampicillin agar plate; then a single colony was transferred to 50 ml of LB medium with 100 μg/ml ampicillin (AppliChem, Darmstadt, Germany) and incubated overnight at 37 °C with shaking (pre-culture). The next day, the pre-culture was used to inoculate 2–4 liters of LB/ampicillin medium. When the A_{600} of the cultures reached 0.7–0.8, protein expression was induced with 1 mM isopropyl β-D-1-thiogalactopyranoside (AppliChem), and the cells were further incubated at 37 °C for 4 h before harvesting by centrifugation at 5000 rpm in a JLA 8.1000 rotor (Beckman Coulter, Bear, CA) for 20 min at 4 °C. Lysis was performed on ice, by resuspending the cell pellet in 40 mM Tris acetate buffer, pH 8.3, containing 1 mM EDTA, 1 mM phenylmethylsulfonyl fluoride (PMSF), and ultrasonicated (VibraCell VCX130, Sonics, Newtown, CT) with an output power of 12 watts applied in 30-s pulses followed by a 30-s pause, for a total ultrasonication time of 5 min. Cell debris were then pelleted by centrifugation at 20,000 rpm in a JA-20 rotor (Beckman Coulter) for 20 min at 4 °C. For the denaturing purification, the supernatant was then boiled at 100 °C in a water bath for 10 min to denature and precipitate most cellular proteins, which are removed by a second centrifugation step (JA-20 rotor, 20000 rpm, 4 °C, 20 min). The boiling step was omitted in the native purification protocol, and the subsequent chromatographic steps were the same for both methods. Lysates were finally filtered through 0.22-μm membranes and applied at 1 ml/min on a HiPrep 16/10 Q FF anion-exchange column connected to an Akta FPLC system (GE Healthcare) and equilibrated with 20 mM Tris, pH 8.0. α-syn was eluted at 3 ml/min by applying increasing concentrations of up to 1.0 M NaCl in 20 mM Tris, pH 8.0, using a linear gradient applied over 10 column volumes. α-syn elutes at ~300 mM NaCl. α-syn-enriched fractions (as determined by SDS-PAGE/Coomassie Blue analysis) were then pooled and further purified by gel-filtration chromatography using a HiLoad 26/60 Superdex 200 column (GE Healthcare) equilibrated with 50 mM Tris, pH 7.5, 150 mM NaCl. Proteins were eluted at 2 ml/min; pure fractions were combined and dialyzed against deionized water at 4 °C using a 7-kDa cutoff dialysis membrane. α-syn purified under denaturing conditions was then flash-frozen in liquid nitrogen and lyophilized. This step was omitted with α-syn purified under nondenaturing conditions, and the protein was kept at 4 °C in a liquid state until use. The A140C mutant was purified similarly to the WT protein (denaturing protocol). A140C α-syn spontaneously forms disulfide-linked dimers during the course of the purification.

Expression and Purification of Recombinant GST-α-syn Fusion Proteins—Protein expression using *E. coli* cells transformed with pGEX-2TK-α-syn and cell lysis were carried out

under nondenaturing conditions (as described above). The GST fusion protein was purified from the bacterial lysate by injection onto a GSTPrep FF 16/10 column at 0.5 ml/min. The binding buffer for the column was a phosphate-buffered saline (PBS) solution (140 mM NaCl, 2.7 mM KCl, 10 mM Na_2HPO_4, 1.8 mM KH_2PO_4), pH 7.3, containing 10 mM DTT and 0.1% v/v Triton X-100. Unbound proteins were washed away with 8 column volumes (CV) of binding buffer, and then the α-syn-GST fusion protein was eluted with 50 mM Tris, pH 8.0, 10 mM DTT, 10 mM reduced glutathione at 1 ml/min. Fractions containing α-syn were further applied to gel-filtration chromatography column (HiLoad 26/60 Superdex 200, same conditions as for the recombinant α-syn monomers). Pure fractions were then subjected to thrombin (GE Healthcare) digestion to remove the GST tag (10 units of thrombin per mg of fusion protein). The cleaved GST tag was then removed by loading the crude cleavage reaction on a GSTrap FF 5-ml (GE Healthcare) equilibrated with the same buffer as described above for affinity purification. The cleaved α-syn was collected in the flow-through and dialyzed against 20 mM sodium phosphate, pH 7.4.

GST-α-synuclein fusion construct in pGEX-4T1 vector was transformed into *E. coli* strain BL21(DE3). Protein expression was performed as described above, except that lysis was performed by six freeze-thaw cycles after resuspending the harvested cells in 50 mM Tris-HCl, pH 7.4, 150 mM NaCl, 2 mM EDTA, 1% Nonidet P-40, 0.1% DTT. Cleared lysates were purified by glutathione affinity chromatography. Removal of the GST tag was also performed similarly as described above.

Lysis of Human RBCs—Erythrocyte concentrates (ECs) from whole blood donations were prepared at the Lausanne Blood Bank (SRTS VD, Epalinges, Switzerland) according to standardized procedures. ECs were stored at 4 °C in sodium/adenine/glucose/mannitol solution. ECs that did not satisfy quality criteria for transfusion were used here. Pelleted RBCs (12 × 15 ml) were lysed by osmotic shock by addition of 31.7 ml of PBS 0.1× plus protease inhibitor mixture (Roche Applied Science) and incubated on a roller for 1 h at 4 °C. After lysis reaction, the supernatants were separated from insoluble material by centrifugation at 17,000 × *g* (30 min, 4 °C) and were transferred to six 50-ml tubes. Supernatants were further ultracentrifuged at 100,000 × *g* for 1 h and 30 min at 4 °C, and the obtained supernatants were filtered with 0.22-μm filters to avoid RBC debris contamination for hemoglobin (Hb) depletion. Supernatants were saved at 4 °C until Hb depletion.

Hemoglobin Depletion—RBC-soluble extracts were Hb-depleted on nickel-based immobilized metal affinity chromatography using a liquid chromatographic BioLogic System from Bio-Rad, based on the method developed by Ringrose *et al.* (21). Soluble extracts were loaded on a nickel-loaded 5-ml HiTrap™ chelating HP or a 20-ml HisPrep™ FF 16/10 column (GE Healthcare) using buffer A (PBS 1×, 10 mM imidazole) at 1 or 3 ml/min, respectively. The Hb-depleted extract passes directly through the column, whereas the Hb is retained until elution with a higher concentration of imidazole. Hb elution was performed by switching the composition of the eluent directly to 100% of buffer B (PBS 1×, 100 mM imidazole). Approximately 95 mg of total proteins were loaded on the 5-ml column, and 400–500 mg were loaded on the 20-ml column at each injection. Hb depletion was quantified according to the Harboe method (22). Hb-depleted fractions were saved at 4 °C for next purification steps.

Nondenaturing Purification of α-syn from Human RBCs—All steps were performed at 4 °C, in the absence of any detergent or denaturant. All buffers were filtered (0.65 μm) and degassed before use. The pH of the Hb-depleted RBC extracts (~350 ml) was first adjusted to 8.0 before loading at 1 ml/min onto a HiTrap™ Q HP 5-ml anion-exchange column equilibrated with 20 mM Tris, 25 mM NaCl, pH 8.0 (ion exchange buffer A). Unbound proteins were washed with 6 CV of IEX buffer A; then weakly bound material was removed by applying 5 CV of 13% of IEX buffer B (20 mM Tris, 1.0 M NaCl, pH 8.0). α-syn was eluted at 1.5 ml/min with a linear gradient from 13 to 100% of ion exchange buffer B over 12 CV, collecting 1.5-ml fractions that were analyzed by SDS-PAGE/Western blot (Syn-1 antibody) and Coomassie staining. α-Syn-positive fractions were pooled for further purification by hydrophobic interaction chromatography (HIC). Pooled IEX fractions were diluted to 50 ml with HIC buffer A (50 mM sodium phosphate, pH 7.0, 1.0 M $(NH_4)_2SO_4$), and the final $(NH_4)_2SO_4$ concentration was adjusted to 1.0 M with powder $(NH_4)_2SO_4$). After filtration (0.22 μm), the solution was loaded at 1 ml/min on a HiTrap™ phenyl FF (high substitution) 1-ml HIC column equilibrated with HIC buffer A. Unbound material was washed with 20 CV of HIC buffer A, and then proteins were eluted (1.5 ml/min) with a linear gradient of 0–100% of HIC buffer B (50 mM sodium phosphate, pH 7.0), during which 750-μl fractions were collected. The column was then washed with 10 CV of HIC buffer B and regenerated with 30 CV of ultra-pure water. Fractions were analyzed by SDS-PAGE/Western blot (Syn-1 antibody) and Coomassie staining; α-syn-containing fractions were concentrated using 5-kDa cutoff Amicon centrifugal concentrators (Millipore, Zug, Switzerland) and run through a final gel-filtration chromatography step on a Superdex 200 10/300 GL column equilibrated with 50 mM Tris, pH 7.5, 150 mM NaCl. 250 μl of concentrated HIC fractions were loaded on each gel-filtration run, and proteins were eluted at 0.5 ml/min while collecting 500-μl fractions. Purity was assessed by SDS-PAGE/silver staining.

Mass Spectrometry—Proteins were analyzed by liquid chromatography-mass spectrometry (LC-MS) on either an LCQ Fleet mass spectrometer or an LTQ system (Thermo Scientific, San Jose, CA). Prior to MS analysis, protein solutions were desalted on line by reversed-phase chromatography on either a Hypersil Gold C_{18} column (4.6 × 150 mm, 5 μm, Thermo, on the LCQ Fleet System) or a Poroshell 300SB C_3 column (1.0 × 75 mm, 5 μm, Agilent Technologies, Santa Clara, CA, on the LTQ system). In both cases, 10-μl samples were injected on the column, and the proteins were eluted with a linear gradient from 5 to 95% of solvent B against solvent A, over 10 min, where solvent A was 0.1% formic acid in ultra-pure water, and solvent B was 0.1% formic acid in acetonitrile. The flow rates were 300 μl/min (LCQ Fleet System) and 500 μl/min (LTQ System). Charge state deconvolution was performed with the MagTran software (Amgen Inc., Thousand Oaks, CA).

NMR Spectroscopy—^{15}N-Labeled recombinant α-syn was obtained from either a denaturing or a nondenaturing purifica-

tion scheme (7). The next steps were conducted as described previously (23). Briefly, $^{1}H/^{15}N$ HSQC data were collected at a protein concentration of 100 μM on a Varian Unity Inova 600-MHz instrument, processed using NMRpipe (24), and analyzed using NMRview (25). Spectra were referenced indirectly to the NMR standards 4,4-dimethyl-4-silapentane-1-sulfonic acid and ammonia (26) using the known chemical shift of water.

Circular Dichroism (CD) Spectroscopy—Proteins were dissolved in CD buffer (10 mM phosphate buffer, pH 7.4) to the final concentrations indicated below. CD spectra were acquired at 20 °C on a J-815 CD spectrometer (Jasco, Tokyo, Japan) in a 1-mm quartz cuvette. Spectra were recorded in the continuous scanning mode (50 nm/min) from 195 to 250 nm with a data pitch of 0.2 nm and a bandwidth of 1 nm. A digital integration time of 2 s was applied. 10 spectra were averaged and smoothed with a Savitzky-Golay filter (convolution width, 25 points). POPG lipid vesicles (100 nm average diameter, prepared by extrusion) were used at 20 mass eq with respect to α-syn for assessment of membrane binding. Lipid/protein mixtures were equilibrated for 30 min at RT before CD spectroscopy.

Analytical Gel Filtration/Static Light Scattering—Samples were applied at 20 μM onto a Superdex 200 10/300 GL column equilibrated with 50 mM Tris, 150 mM NaCl, 0.05% w/v NaN_3, pH 7.5, and eluted at 0.5 ml/min using an Agilent 1200 series HPLC pump (Agilent, Santa Clara, CA). Protein detection was done by monitoring absorbance at 280 nm (Agilent 1200 VWD). Absolute molecular weights were determined by static light scattering using a Wyatt Dawn Heleos II multiangle light scattering detector (Wyatt Technology Europe GmbH, Dernbach, Germany) connected in series with the UV detector. The protein concentration data used to obtain molecular weights from light scattering data were derived from refractive index measurements (Wyatt Optilab rEX, connected downstream of the LS detector). The standard value of $dn/dc = 0.185$ ml/g for proteins was used.

Cell Culture and Transient Transfection—Human embryonic kidney cells (HEK293T) and HeLa cells were maintained in culture with Dulbecco's modified Eagle's medium (DMEM, Invitrogen) supplemented with 10% fetal bovine serum (FBS) and 5% penicillin/streptomycin. Human neuroblastoma SH-SY5Y cells and stably transfected SH-SY5Y-expressing α-syn WT were obtained from SISSA (Neurobiology Sector Ed, Q1 Area Scientific Park, Basovizza; Italy) and cultured in Ham's F-12 + minimum Eagle's medium supplemented with essential amino acids and 10% FBS. Chinese hamster ovary (CHO) cells were kindly provided by the Markram laboratory (EPFL, Switzerland). All the media were enriched with 1% penicillin/streptomycin, and the cells were grown in 150-cm^2 flasks (TPP®, Trasadingen, Switzerland) in a humidified incubator (5% CO_2, 37 °C). The transient transfection of 10 μg of DNA in HEK293T and HeLa cells was performed on 100-mm dishes at a cell density of 70–80%, using the standard calcium phosphate ($CaPO_4$) and Lipofectamine™ transfection protocols, respectively.

Cell Lysis, Protein Extraction, and Protein Assay—After 72 h of culture, the cells were harvested and lysed by osmotic shock in either 20 mM Tris, pH 7.4, or PBS, both containing 1× protease inhibitor mixture P3840 (Sigma) and 1 mM PMSF and then passed mechanically through a 0.5 × 16-mm needle several times before sonication (pulse 3 s on and 3 s off, 65% amplitude). Lysates were then cleared by centrifugation of the mixture (14,000 × *g*, 15 min, 4 °C), and supernatants were transferred in new tubes. The total amount of protein in the total lysate was estimated with the BCA™ protein assay kit from Thermo Scientific, according to the manufacturer's instructions.

In-cell Cross-linking—Cells were harvested and washed twice with ice-cold 1× PBS, pH 7.4. Disuccinimidyl suberate ligand (Pierce) was solubilized in DMSO to an initial concentration of 100 mM. The aliquot was then added to the cells to a final concentration of 2.5 and 5 mM in a total reaction volume of 100 μl. After a 30-min incubation at room temperature, the reaction was quenched by addition of 1 M Tris base solution to a final concentration of 20 mM. The cells were then lysed in 20 mM Tris base, pH 7.4, containing 150 mM NaCl, 1 mM EDTA, 0.25% Nonidet P-40, 0.25% Triton X-100, 1 mM PMSF (Sigma) and 1:200 protease inhibitor mixture (Sigma). Insoluble particles were pelleted by centrifugation at 14,000 × *g* for 10 min at 4 °C.

Native-PAGE—Clear Native-PAGE (CN-PAGE) was performed on 7.5% acrylamide homemade Clear Native-PAGE (60), with a constant current of 25 mA for ~2 h. Briefly, the resolving gel was obtained by mixing 20% of 40% aqueous acrylamide:bisacrylamide (37.5:1) (AppliChem) with 25% of 1.5 M Tris, pH 8.8, and 56% of double distilled water, and the stacking gel was prepared by mixing 10% of a 40% aqueous acrylamide: bisacrylamide (37.5:1) solution, 25% of 0.5 M Tris, pH 6.8, and 65% of double distilled water. Blue Native-PAGE was performed using Novex® 4–12% gradient gels. The samples were prepared by addition of 5% Coomassie G-250 additive. Standard proteins were loaded using NativeMark Unstained Protein Standard (Invitrogen). Blue Native-polyacrylamide gels were then run at 130 V for 1 h according to the manufacturer's protocol. For Western blot analysis, proteins were transferred onto PVDF membranes (0.2 μm pore size, Bio-Rad).

Primary Antibodies—The following antibodies were used in this study: anti-human specific antibody against α-syn (Syn-211 clone), epitope 121–125 (sc-12767), as well as the nonhuman specific FL-140, epitope 61–95 (sc-10717) (27), were purchased from Santa Cruz Biotechnology, Inc. (Santa Cruz, CA). The Syn-1 antibody (epitope 91–99 (28)) was obtained from BD Pharmingen. The anti-β-actin antibody was from Abcam (Cambridge, MA). The rabbit polyclonal antibody SA-3400 (epitope 117–131, recognizes human and rat α-syn) was purchased from Enzo Life Sciences (Farmingdale, NY). Finally, the goat polyclonal antibody N-19 (recognizes the N-terminal region of α- and β-syn) was obtained from Santa Cruz Biotechnology, Inc.

SDS-PAGE and Immunoblotting—Samples were diluted in loading buffer and separated on homogeneous 15% SDS-polyacrylamide gels (1.5 mm thickness). The electrophoresis and Western blot were conducted as described previously (29). For the detection of endogenous levels of α-syn, we employed an enhanced chemiluminescence (ECL) detection method. Briefly, PVDF or nitrocellulose membranes were blocked in 5% nonfat dried milk powder (AppliChem) in PBS for 30 min. The blot was then incubated overnight at 4 °C with primary antibody diluted in the antibody solution (5% milk in PBS 0.1% Tween

20). After four washes with PBS, 0.1% Tween 20 (PBST), the membrane was incubated for 1 h at room temperature (RT) with the HRP-conjugated secondary antibody (anti-mouse or anti-rabbit from The Jackson Laboratory) diluted 1:7500 in antibody solution. After four washes in PBST and three washes in PBS, the substrate mixture (SuperSignal® West Pico Chemiluminescent Substrate, Pierce) was added to the membrane and incubated for 5 min at RT. Revelation was then performed by exposing FUJI medical x-ray films to the substrate-treated membranes in a dark room.

Immunoassay for α-syn Oligomers—An ELISA 384-well plate (Nunc Maxisorb, Nunc, Denmark) was coated by overnight incubation at 4 °C with 1 μg/ml of mouse monoclonal antibody (mAb) Syn-211 (Santa Cruz Biotechnology) in 200 mM $NaHCO_3$, pH 9.6 (50 μl/well). Then the plate was washed four times with PBST and incubated then with 100 μl/well of blocking buffer (5% gelatin from cold water fish skin, 0.05% Tween 20 in PBS, pH 7.4) for 2 h at 37 °C. After washing four times with PBST, 50 μl of the samples to be tested were added in duplicate and then incubated at 37 °C for another 3 h. Biotinylated Syn-211 diluted to 1 μg/ml in blocking buffer was added after washing with PBST and incubated at 37 °C for 2 h. The plate was washed and then incubated for 1 h at 37 °C with 50 μl/well of ExtrAvidin-Peroxidase (Sigma). The plate was washed and then incubated with 50 μl/well of an enhanced chemiluminescent substrate (Super-Signal ELISA Femto, Pierce), after which chemiluminescence in relative light units was immediately measured with a Victor^3 1420 (Wallac) microplate reader.

Immunoassay for Total α-Synuclein—Total α-synuclein levels in different cell lysate samples were measured using a sandwich ELISA. In brief, the anti-human α-synuclein mAb Syn-211 (Santa Cruz Biotechnology) was used for capturing, and the anti-human α-synuclein polyclonal antibody FL-140 (Santa Cruz Biotechnology) was used for antigen detection through a horseradish peroxidase (HRP)-linked chemiluminescence assay. The 384-well ELISA plate (Nunc Maxisorb, NUNC, Denmark) was coated with 1 μg/ml Syn-211 (50 μl/well) in 200 mM $NaHCO_3$, pH 9.6, and incubated overnight at 4 °C. After washing four times with PBS containing 0.05% Tween 20 (PBST) and incubating for 2 h with 100 μl/well of blocking buffer (PBS containing 5% gelatin and 0.05% Tween 20), 50 μl of the cell lysate samples were then added to each well and incubated at 37 °C for 3 h. Captured α-synuclein protein was detected by 0.2 μg/ml of FL-140 (50 μl/well), followed by incubation with 50 μl/well (1:5,000 dilution in blocking buffer) of HRP-labeled anti-rabbit antibody (The Jackson Laboratory). Bound HRP activity was assayed by chemiluminescent reaction using an enhanced chemiluminescent substrate (SuperSignal ELISA Femto, Pierce). Chemiluminescence in relative light units was immediately measured with a Victor^3 1420 (Wallac) microplate reader. The standard curve for the ELISA was carried out using 50 μl/well of recombinant human α-synuclein solution at different protein concentrations in blocking buffer.

Preparation of α-syn Aggregates—"Aged" α-syn samples that were used in the ELISAs were prepared as follows. 1 ml of 50 μM purified α-syn in PBS, pH 7.4, with few drops of mineral oil on top was incubated at 37 °C in parafilm-sealed, 1.5-ml Eppendorf tubes for 7 days in a Thermomixer (Eppendorf) with continuous mixing at 800 rpm.

Extraction of Native α-syn from Transgenic Mouse Brains—Transgenic mice expressing A53T human α-syn under the control of the mouse prion protein promoter (kindly provided by Dr. Michael K. Lee, University of Minnesota) were used in this analysis to investigate the conformation of the human protein expressed endogenously in the nervous system. This disease model demonstrates progressive late-onset neurodegeneration accompanied by pathological changes and α-syn inclusion formation in selective brain regions such as the brainstem, whereas other regions such as the cortex remain largely unaffected (21). Frontal cortex and brainstem were dissected from A53T transgenic mice (30) and nontransgenic littermate control mice at 6 months of age (no apparent motor phenotype at the time that the mice were sacrificed). Tissues were homogenized briefly with the aid of a mechanical homogenizer in 50 mM HEPES buffer, pH 7.4, containing phosphatase inhibitors, mixtures 2 and 3 (Sigma), and complete protease inhibitor mixture (Roche Applied Science). Following homogenization, the samples were subjected to ultracentrifugation at 100,000 × *g* for 20 min at 4 °C, and protein concentration was determined in the supernatants by BCA assays (Pierce). The samples were maintained on ice at all times during preparation, avoiding freezing and thawing steps. Brains from transgenic mice overexpressing WT human α-syn under the control of the *mThy1* promoter that were first described by Rockenstein *et al.* (31) were also analyzed. The mThy1-α-syn transgenic mice were selected because they display more extensive α-syn accumulation in the frontal cortex, limbic system, and subcortical regions, including the basal ganglia and the substantia nigra pars compacta (SNpc). Harlan strain C57BL/6JRccHsd (WT) and C57BL/6JOlaHsd α-syn-deficient mice (α-synKO) were obtained from The Jackson Laboratory (ID:003692). For the immunoblot, a total of 12 6-month-old mice were used ($n = 4$ non-TG; $n = 4$ mThy1-α-syn TG, and $n = 4$ -α-syn knock-out mice).

Recombinant AAV2/6 Production and Titration—Recombinant pseudotyped AAV2/6 vectors were produced, purified, and titrated as described previously (32). Briefly, we measured by real time PCR the number of transcriptionally active double-stranded transgene copies at 48 h in HEK293T cells and obtained a titer of 7.9×10^{10} titer units/ml for the AAV2/6-PGK-α-syn-WT vector.

Stereotaxic Unilateral Injection into Rat Substantia Nigra and Tissue Processing—Female adult Sprague-Dawley rats (Charles River Laboratories, l'Arbresle, France), weighing ~200 g, were housed in a 12-h light/dark cycle, with *ad libitum* access to food and water, in accordance with Swiss legislation and the European Community Council directive (86/609/EEC) for the care and use of laboratory animals. For stereotaxic injections, the animals were deeply anesthetized with a mixture of xylazine/ketamine prior to placement in a stereotaxic frame (David Kopf Instruments, Tujunga, CA). Two μl of viral preparation were injected in the right brain hemisphere using a 10-μl Hamilton syringe with a 34-gauge blunt tip needle connected to an automatic pump (CMA Microdialysis, Solna, Sweden) at a speed of 0.2 μl/min. The needle was left in place for an

additional 7 min before being slowly withdrawn. For transducing the SNpc, the following coordinates were used: anteroposterior, −5.2 mm; mediolateral, −2.0 mm relative to bregma; dorsoventral, −7.8 mm relative to skull surface. The vector AAV2/6-PGK-α-syn-WT was unilaterally injected at a total dose of 2.8×10^7 titer units.

Rats were sacrificed by decapitation, and the striatum and substantia nigra were dissected from both hemispheres and immediately frozen in liquid nitrogen. For native gel separation, proteins were extracted using an Ultra-Turrax® homogenizer (Ika, Staufen, Germany) in detergent-free buffer: HEPES 50 mM, pH 7.4, NaCl 150 mM, supplemented with Roche PhosphoStop and Roche Mini Complete protease inhibitor according to manufacturer's instructions (Hoffmann-La Roche). Extraction volume was 100 μl per substantia nigra and 250 μl per striatum. Finally, the samples were centrifuged at 200,000 × *g* for 20 min, and the supernatants were collected. All extraction steps were performed at 4 °C.

Isolation and Characterization of α-syn from Human Tissues—A total of 18 human cases were included for this study. These were divided into three groups as follows: control (neurologically unimpaired), Alzheimer disease (AD), and dementia with Lewy bodies (DLB). The autopsy cases in this study came from patients evaluated at a number of sites associated with the Alzheimer Disease Research Center at the University of California, San Diego. Written informed consent for neurobehavioral evaluation, autopsy, and for the collection of samples and subsequent analysis was obtained from the patient and caregiver (usually the next of kin) before neuropsychological testing and after the procedures of the study had been fully explained. The study methodologies conformed to the standards set by the Declaration of Helsinki and Federal guidelines for the protection of human subjects. All procedures were reviewed and approved by the University of California, San Diego, Institutional Review Board. The diagnosis of DLB was based in the initial clinical presentation with dementia followed by parkinsonism and the presence of α-syn and ubiquitin-positive LBs in cortical and subcortical regions (33).

As described previously (34), frontal cortex from human and mouse brain samples (0.1 g) were homogenized in 0.7 ml of buffer B (1.0 mM HEPES, 5.0 mM benzamidine, 3.0 mM EDTA, 0.5 mM magnesium sulfate, 0.05% sodium azide; final pH 8.8) containing phosphatase and protease inhibitor mixtures (Calbiochem). Samples were centrifuged at 5000 × *g* for 5 min at room temperature. Supernatants were retained and placed into appropriate ultracentrifuge tubes and centrifuged at 100,000 × *g* for 1 h at 4 °C. This supernatant was collected to serve as the cytosolic fraction. The BCA protein assay was used to determine the protein concentration of the samples.

RESULTS

Although gel electrophoresis and size-exclusion chromatography do not allow for accurate determination of protein molecular weight, especially in the case of natively unfolded proteins, these techniques remain the most accessible and commonly used to estimate the size and oligomeric states of proteins in complex mixtures. In these techniques, the behavior of proteins is dependent not only on the size but also on the charge and conformational states (shape) of the protein. Therefore, the use of globular proteins as calibration standards may not be appropriate for the characterization of unfolded proteins such as α-syn. To allow more accurate assessment and comparison of the oligomeric state of α-syn derived from different sources, the following protein standards of well-defined chemical integrity and purity (assessed by SDS-PAGE and mass spectrometry), as well as conformational properties (measured by CD) and oligomeric state (determined by size-exclusion chromatography coupled to light scattering) were generated and used as controls in all the studies presented below: 1) unfolded monomeric α-syn from *E. coli*; 2) disulfide-linked α-syn dimer (A140C mutation) produced in *E. coli*; and 3) α-syn specifically acetylated at the N terminus. Unlike α-syn produced in *E. coli*, the majority of α-syn expressed in the brain and in mammalian cell lines undergoes N-terminal acetylation (35, 36). Direct comparison of these standards and native α-syn from different sources on the same gel is particularly important, because the migration profile of a given protein in native gel electrophoresis is dependent on its molecular weight, conformation and charge state, as well as the percentage of acrylamide within the gel.

Recombinant WT Human α-syn Produced in E. coli and Purified under Native or Denaturing Conditions Exists as a Disordered Monomer—Purified recombinant α-syn purified from *E. coli* is commonly used as a standard and is the main form of α-syn used for all biophysical studies to assess the effect of mutations, post-translational modifications, protein-ligand and protein-protein interactions on the biochemical, structural, and aggregation properties of α-syn *in vitro*. Since the first observation that α-syn is a thermostable protein (37, 38), most recombinant α-syn purification protocols included a denaturing heating step to remove the majority of heat-labile cellular proteins, a pre-purification step performed before further purification by chromatographic separation techniques such as ion-exchange and size-exclusion chromatography. In some cases, a final purification step using reversed-phase chromatography is introduced to prepare highly pure protein (23). It has recently been suggested that these procedures may have caused the mischaracterization of the native state of α-syn (1, 2). Therefore, we first sought to determine whether this heating step affects the structure of recombinant α-syn purified from *E. coli.* As such, bacterial lysates (obtained by gentle ultrasonication, without the use of any detergent) were either directly filtered through 0.22-μm membranes (native, nondenaturing protocol) or boiled in a water-bath at 100 °C for 10 min and centrifuged (denaturing protocol). Cleared lysates from both samples were then purified by anion-exchange followed by gel-filtration chromatography. Interestingly, α-syn from both denaturing and nondenaturing preparations eluted at the same volume on the Superdex 200 26/60 gel-filtration column (~200 ml), suggesting that both share a similar Stokes radius. Mass spectrometry (ESI-MS) analysis of both purified native and denatured α-syn showed an identical mass (Fig. 1*A*). The deconvoluted masses were 14,457 Da (native protocol) and 14,461 Da (denaturing protocol), which are within the instrument's measurement error for an expected mass of 14,460 Da. Purity of these samples was further confirmed by SDS-PAGE,

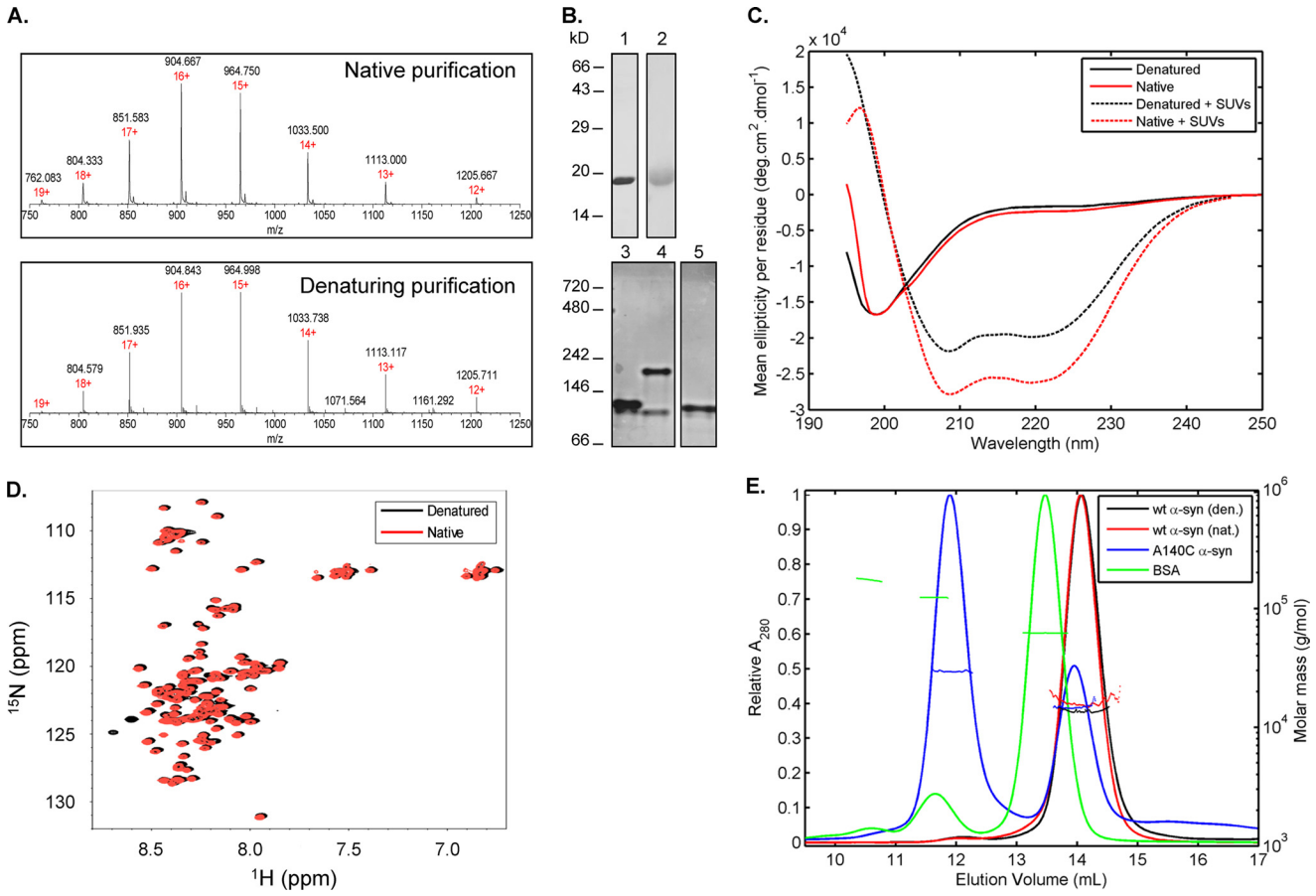

FIGURE 1. **Nondenatured and denatured recombinant WT α-syn exists as an unfolded monomer.** *A,* ESI-MS spectra of purified native WT α-syn (*top panel*) and α-syn obtained using a boiling protocol (*bottom panel*). *Numbers* above the peaks indicate charge states. *B,* SDS-PAGE (*top panel*) and CN-PAGE (*bottom panel*) analyses of purified recombinant proteins. *Lane 1*, boiled WT α-syn; *lane 2,* native WT α-syn; *lane 3*, boiled WT α-syn (CN-PAGE); *lane 4,* A140C α-syn (CN-PAGE); *lane 5,* native WT α-syn (CN-PAGE). *C,* CD spectra of boiled (*black*) WT α-syn and native (*red*) WT α-syn in absence (*continuous lines*) and presence (*dashed lines*) of 100 nm of extruded POPG small unilamellar vesicles (5 mass eq.). *D,* ^{1}H-^{15}N HSQC spectra of denatured (*black*) *versus* native (*red*) WT ^{15}N-labeled α-syn at 100 μM. *E,* analytical gel filtration/light scattering profiles of boiled (*black*) *versus* native (*red*) α-syn. A mixture of A140C α-syn monomers and dimers (*blue*) and BSA (*green*) was used as control. *Continuous lines* correspond to normalized absorbance (280 nm, *left ordinate axis*), and *thin line* segments correspond to the calculated molar masses for the corresponding absorbance peaks (*right ordinate axis*).

which showed that both proteins migrate as single bands with an apparent mass of ~19 kDa (Fig. 1*B*, *top panel*).

Far-UV CD spectroscopy performed at a protein concentration of 5 μM revealed that both native and heat-treated recombinant α-syn were mostly devoid of any significant secondary structure, as shown by a single spectral minimum at ~195 nm (Fig. 1*C*). Moreover, we confirmed that both native and denatured preparations are able to bind lipids and adopt an α-helical structure upon binding to 100-nm POPG small unilamellar vesicles. Because CD spectroscopy only detects quite substantial conformational changes and is not sensitive to minor differences in tertiary structure, we further probed the structural similarity between native and denatured recombinant α-syn, by using the much more sensitive technique of NMR spectroscopy. ^{15}N-Labeled proteins were obtained from expression in minimal medium as described previously (23). Denatured α-syn was obtained using a protocol that included reversed-phase HPLC purification as a last step. It must be noted that for this sample, the commonly used boiling protocol was not applied. Denatured α-syn was compared with a sample purified without exposing the protein to any denaturing conditions. As presented in Fig. 1*D*, the NMR spectra of α-syn obtained for the two different purification procedures are nearly identical, and both clearly indicate the highly disordered conformational ensemble that was originally documented (23) and has since been extensively studied by us (39–46) and many other groups (47–53).

We then characterized the quaternary structure of recombinant proteins obtained under both native and denaturing conditions by analytical gel-filtration chromatography/static light scattering, which measures the absolute weight-average molecular mass of proteins. Both native and heat-treated recombinant α-syn proteins co-eluted at ~14 ml on the Superdex 200 10/300 GL column and showed the same molecular mass of 14 ± 1 kDa (Fig. 1*E*), which is strongly indicative of a monomeric state. The A140C α-syn dimeric mutant eluted as two species as follows: the major one at ~12 ml was confirmed to be dimeric by light scattering (observed molecular mass, 29.6 ± 0.4 kDa), and a second less abundant species that co-eluted with WT recombinant α-syn had a measured molecular mass of 14.9 ± 0.7 kDa, consistent with a monomeric state. The system was correctly calibrated, as shown by the chromatogram of BSA (measured monomer molecular mass, 62.2 ± 0.1 kDa) for which dimers and trimers eluting at ~11.6 and ~10.6 ml,

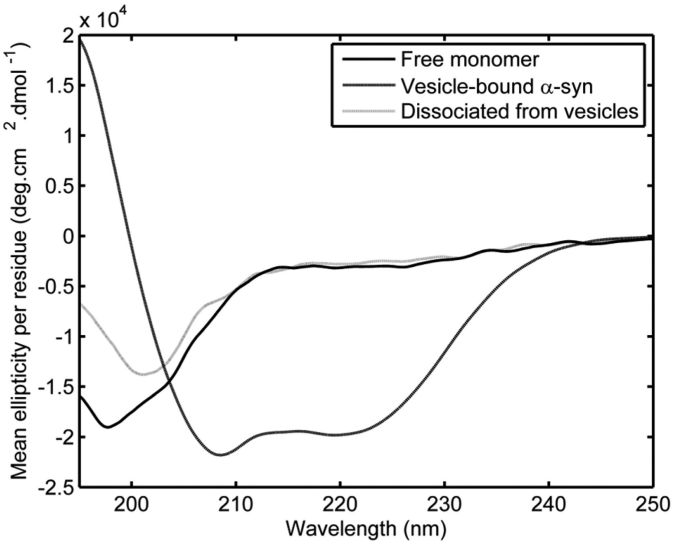

FIGURE 2. **Membrane-bound α-syn does not keep its α-helical conformation once dissociated.** CD spectra were taken without (*continuous line*) and with (*dashed line*) 5 mass eq. of 100 nm of extruded POPG vesicles. Membrane-bound α-syn was dissociated by adding NaCl to a final concentration of 1 M; then vesicles and any remaining membrane-bound α-syn were removed by filtration through 100-kDa cutoff membranes. The filtrate represents dissociated α-syn (*dotted line spectrum*).

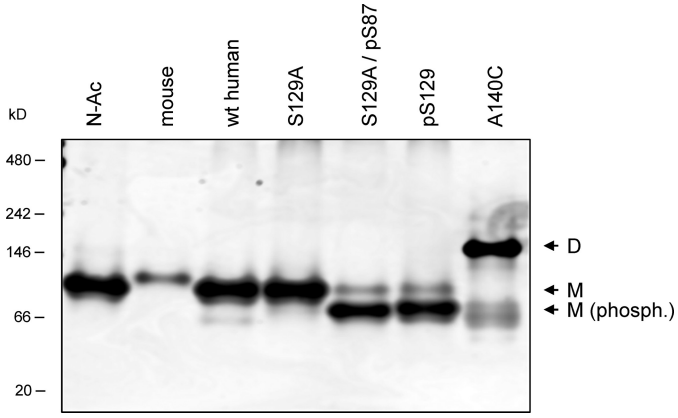

FIGURE 3. **Comparison of electrophoretic mobility of different α-syn variants on CN-PAGE.** Recombinant proteins were purified as described under "Experimental Procedures," and then resolved on a 7.5% clear native gel. Addition of negative charge at Ser-87 or Ser-129 increases the mobility of α-syn. Unmodified α-syn migrates at above 66 kDa. *M*, α-syn monomers; *D*, α-syn dimers. *N-Ac*, *N*-acetylated α-syn; *M* (*phospho*), phosphorylated α-syn monomer.

respectively, were also observed with the expected molecular mass. It is noteworthy that monomeric BSA elutes at a position very close to monomeric α-syn, suggesting a similar Stokes radius, despite the large difference in molecular weight between the two proteins. This observation is consistent with previous studies demonstrating that unfolded monomeric α-syn shows a Stokes radius of 29–34 Å due to its unfolded elongated structure (6, 44).

It has been suggested that the failure of recombinant α-syn to adopt any stable secondary structure could be due to the absence of necessary co-factors or machinery needed for its correct folding in *E. coli* (1). An alternative explanation would be that recombinant unfolded α-syn represents a kinetically trapped form of the protein. Therefore, we tried to assess if overcoming this barrier by using other factors to induce α-helical structure in α-syn would lead to the formation of a stable secondary structure. Toward this, we investigated if membrane-bound α-syn would retain its α-helical rich structure after dissociation from the membranes. We hypothesized that membrane-bound α-syn should retain its α-helical rich structure after disassociation from the membrane by addition of a high salt concentration. After addition of 1 M NaCl, the released α-syn was recovered by filtering the sample through a 100-kDa cutoff filter. Upon reassessment of the free α-syn (flow-through) conformation by CD, we observed that the protein had lost its α-helical structure and had become unstructured again (Fig. 2).

Probing the Distribution of α-syn Species Using Native Gel Electrophoresis Techniques—Because native and denaturing gel electrophoresis remain the primary techniques used to assess the distribution of quaternary structures of α-syn in complex mixtures from cells or brain tissue lysates, we sought to determine whether denaturation by boiling would affect the migration pattern of recombinant or endogenously expressed α-syn on native gels. Interestingly, both native and heat-treated recombinant α-syn co-migrated at an estimated molecular mass of >66 kDa in clear native gels (homogeneous gel, 7.5% acrylamide in the resolving section) (Fig. 1*B*, *bottom panel*). To determine to what extent native gels can differentiate between different sequence and oligomeric variants of α-syn, we compared the migration of recombinant: (i) monomeric N^{α}-acetylated human α-syn; (ii) monomeric human and mouse α-syn; (iii) monomeric and phosphorylated α-syn at Ser-87 or Ser-129; and (iv) a disulfide-linked dimeric form of the protein (A140C). Fig. 3 demonstrates that the disulfide-linked dimeric form of α-syn migrated significantly slower than the WT protein. The phosphorylated forms of α-syn (at Ser-87 or Ser-129) migrated slightly faster than the WT. Recombinant mouse α-syn migrated at a slightly higher position than the corresponding human protein. Murine α-syn differs from the human protein by seven residues and has a slightly higher molecular weight (14,485 Da) than human α-syn (14,460 Da). Given the small difference in mass between the two proteins, it is plausible that the observed difference in mobility is attributed mainly to the loss of one negative charge (because of the D121G substitution in murine α-syn) and/or conformational properties of the proteins rather than the small difference in molecular weight. Importantly, N-terminal acetylation does not significantly affect the migration of the human protein in native gels, even though it decreases the net charge of the protein by 1 unit. Boiling of the samples before loading did not change their electrophoretic mobility (supplemental Fig. S1). These results suggest that native gels could potentially provide a reliable method for detecting and differentiating between different oligomeric states and modified forms of α-syn in complex mixtures but do not provide an accurate estimate of the size and quaternary structure distribution of α-syn.

Native α-syn from Mouse and Rat Brains Exhibits Similar, Properties as the Unfolded Recombinant Monomers—Using native gels and the well characterized standards described above, we assessed the quaternary structure distribution of native α-syn expressed in mouse and rat. As such, the electro-

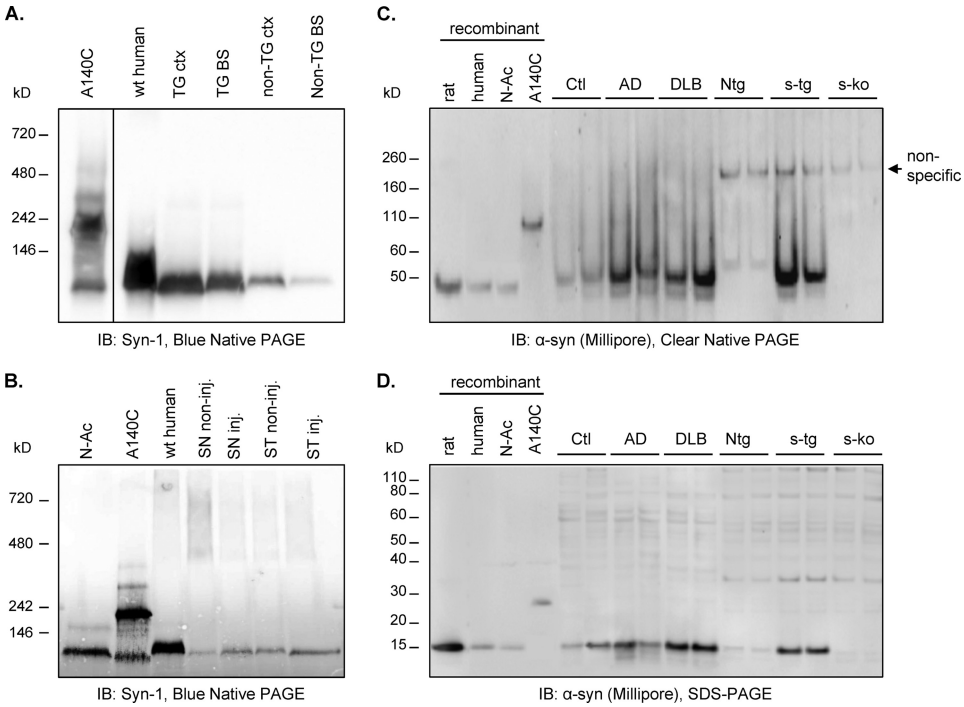

FIGURE 4. **Native α-syn from *in vivo* sources co-migrates with recombinant unfolded α-syn monomer.** *A,* CN-PAGE analysis of nontransgenic and transgenic (expressing A53T human α-syn) mouse brain homogenates (10 μg of total protein per lane) extracted under nondenaturing conditions. 200 ng of recombinant standards were used. The blot was probed using the Syn-1 clone antibody that recognizes both human and mouse α-syn. Immunodetection was performed using ECL (GE Healthcare) chemiluminescence detection reagent. Images were captured using a FujiFilm LAS-4000 luminescent image analysis system. *ctx,* cortex; *BS,* brain stem. *B,* same experiment was performed from rat brain homogenates obtained 4 weeks after AAV injection as described under "Experimental Procedures." 10 μg of total protein were also loaded on each lane. Western blots were processed as in *A*. *SN,* substantia nigra; *ST,* striatum; *inj*, injected. *C,* CN-PAGE of native α-syn from human control and diseased brains, an independent mouse transgenic line, and α-syn-KO (*s-ko*) mice (negative control). For analysis in clear native gels, 18 μg of total protein (from mouse and human brain homogenates) were prepared in Novex Tris-glycine (*Ntg*) native sample buffer (Invitrogen) and separated by gel electrophoresis on 12% Tris-glycine gels (Invitrogen). Blots were incubated overnight at 4 °C with antibodies against α-syn (Millipore). Membranes were processed using a chemiluminescence kit (Western Lightning Chemiluminescence Reagent Plus; PerkinElmer Life Sciences) and imaged using a Versadoc system (Bio-Rad). The *arrow* marks nonspecific bands (assigned as such because they appear in α-syn-KO mouse samples). *Ctl*, control. *D,* SDS-PAGE analysis of the same samples as in *C*. Samples were heated for 10 min at 70 °C and then separated by gel electrophoresis on 4–12% BisTris SDS-polyacrylamide gels (Invitrogen). Western blots were also processed in the same way as in *C*. *IB*, immunoblot; *N-Ac*, *N*-acetylated α-syn.

phoretic mobility of endogenous α-syn from these samples was assessed using native and denaturing gel electrophoresis. To preserve the native conformation of the proteins and to prevent breakdown of potential higher protein assemblies, the lysis buffer used to homogenize the tissues was free of detergents and denaturing agents. Lysates obtained from the cortex and brainstem regions of 6–7-month-old (pre-symptomatic) A53T α-syn transgenic mice and their nontransgenic littermates were loaded on Blue Native 4–12% polyacrylamide gradient gels along with the protein standards described above. Immunoblotting with the α-syn-specific antibody Syn-1 (which detects both human and mouse α-syn) revealed that α-syn from transgenic mouse brain tissues migrates with an apparent molecular mass of >66 kDa and co-migrates with the unfolded monomeric standards (Fig. 4*A*), but below the dimeric A140C α-syn. The endogenous murine α-syn also migrated similarly. SDS-PAGE showed that all samples (with the exception of A140C α-syn) were monomeric under denaturing conditions (supplemental Fig. S2*A*).

We then tried to perform denaturation assays of native murine brain-derived α-syn by heating the lysates, followed by resolution on CN-PAGE and Western blot analysis (supplemental Fig. S1*C*). However, heat-induced denaturation resulted in very broad smearing bands migrating more slowly than the nonheated samples. The same effect was observed when exogenous monomeric (recombinant) α-syn was added to brain homogenates from α-syn KO mice before heating, suggesting that the observed smears are due to co-precipitation of α-syn with other denatured proteins from the lysates.

In addition, we performed similar analyses on brain homogenates obtained from rats infected with AAV2/6 vectors driving the expression of WT human α-syn as described previously (32). Viral vectors were delivered by stereotaxic injection into the SNpc, and biochemical analysis was carried out 4 weeks post-injection. Contralateral (*i.e.* noninjected) striatum and SNpc homogenates were included in our analyses as controls to allow comparison with the overexpressed human α-syn. The total α-syn level in the injected hemisphere was higher than in the noninjected hemisphere, although to a much lower extent than in transgenic mice (see Fig. 4*A*), consistent with previous reports using the same model system (54). Interestingly, rat and overexpressed human α-syn in both SNpc and striatum co-migrated again with the same apparent molecular weight as the unfolded, monomeric standards on Blue Native 4–12% gels (also at an apparent molecular weight >66 kDa (Fig. 4*B*)) and SDS-PAGE (supplemental Fig. S2*B*). Note that the 20- and 66-kDa bands of the molecular weight standard were not detected in experiments involving rat and mouse brains, because Blue Native-PAGE results in the lower parts of the membrane being stained. Together, these results suggest that

α-syn from mouse and rat brains exhibit similar apparent size, charge, and conformational properties as the unfolded monomeric recombinant α-syn.

As an alternative method to detect potential oligomeric forms of α-syn in rodent brains, we applied wild-type C57BL/6J mouse brain homogenates (prepared in denaturant-free conditions) onto a Superdex 200 gel-filtration column. The elution pattern of α-syn was then assessed by Western blotting against α-syn from the collected fractions (supplemental Fig. S3*A*), which was compared with the elution of recombinant monomeric human α-syn alone and to that of recombinant monomeric human α-syn spiked into brain homogenates obtained from C57BL/6JRccHsd α-syn-KO mice (Harlan, Netherlands) (supplemental Fig. S3*B*). As expected, native brain-derived murine α-syn eluted at the same position as the unfolded recombinant monomer. The same result was obtained when the recombinant monomer was added into the α-syn-KO mouse brain lysates (supplemental Fig. S3*B*).

Human α-syn from Post-mortem Human Brains and Monomeric Unfolded Recombinant Co-migrate on Native and Denaturing Gel Electrophoresis—Finally, we wanted to assess the state of native α-syn in post-mortem human brains from healthy controls, patients with AD, and patients affected with DLB. Samples were obtained and processed under nondenaturing conditions as described under "Experimental Procedures." Immunoblot analysis in SDS-PAGE (Fig. 4*D*) gels of samples from human brains showed that α-syn is identified in the soluble fractions primarily as a ~14-kDa protein that appears more abundant in the brains of the DLB cases compared with controls and AD cases. Then, CN-PAGE was performed. To allow direct comparison with native α-syn, all the samples were loaded on the same gels. As shown in Fig. 4*C*, overexpressed human α-syn was detected in the brains of α-syn TG mice. Human brain-derived α-syn migrated at ~50 kDa, at the same position as the unfolded recombinant protein and α-syn from transgenic mice. The discrepancy between the apparent molecular weights obtained in this experiment and the others (where α-syn migrated between the 66 and the 146 kDa standards) can be explained by the different gel systems used (homogeneous 12% here, and homogeneous 7.5% or 4–12% gradient gels in the other experiments). However, the key observation that native α-syn co-migrates with recombinant monomeric controls holds in all experiments performed in our studies. Thus, the dependence of the apparent molecular mass upon the type of gels used is further evidence that molecular weight estimation using Native-PAGE is not reliable. Note that endogenous mouse α-syn (from the non-TG mice) migrated slightly slower than the human protein from TG mice. This is a property of the mouse α-syn itself, which is also seen when recombinant mouse α-syn is run on Native-PAGE (see Fig. 3). These results demonstrate that in native gels (Fig. 4*C*) α-syn from human, rat, and mouse brains exhibit virtually identical migration and apparent molecular weight as the unfolded monomeric α-syn.

Together, these results suggest that native α-syn exists as a monomer in the brain, which is in contrast to the recent reports suggesting that native α-syn isolated from human red blood cells, mammalian cell lines, or *E. coli* exists as a stable tetramer. To allow direct comparison with previous results, we also assessed the quaternary structure distribution of α-syn in RBCs and mammalian cell lines (HEK293, HeLa, SH-SY5Y, CHO, and COS-7 cell lines) relative to the conformationally and hydrodynamically defined α-syn standards described above.

Native α-syn from Various Cell Lines Co-migrates with Recombinant Unfolded Monomers on Native-PAGE and Co-elute in Size-exclusion Chromatography—We compared the migration of overexpressed and endogenously expressed α-syn in five different mammalian cell lines (HEK293T, HeLa, COS-7, SH-SY5Y, and CHO K1) using denaturing (SDS-PAGE) and nondenaturing (CN-PAGE) gels. It is noteworthy that endogenous α-syn could not be detected using fluorescence detection (Alexa Fluor-conjugated secondary antibodies) methods (Fig. 5*A*) but could be observed using enhanced chemiluminescence upon loading 200 μg of total protein lysate (Fig. 5*B*). Similar to α-syn extracted from mouse, rat, and human brains, native α-syn from HEK, HeLa, and SH-SY5Y cell lines (both endogenous and overexpressed levels) showed similar electrophoretic mobility as the unfolded monomeric standards on SDS-PAGE (Fig. 5, *A* and *B*) and CN-PAGE (Fig. 5, *C* and *D*). No other (oligomeric) species were observed under these conditions. Note that α-syn obtained from COS-7 cells consistently migrated at a slightly higher level than expected on CN-PAGE but always below the dimeric standard. Although the α-syn sequence corresponding to the African green monkey from which COS-7 cells are derived is not available, the α-syn sequence of the closely related primate *Erythrocebus patas* suggests a single amino acid substitution (E114Q) within the C-terminal domain of the protein, which shifts the net charge of the protein by +1, which would in turn be expected to slow down α-syn migration on CN-polyacrylamide gels.

These findings were confirmed by size-exclusion chromatography, which showed that native α-syn or human α-syn expressed in HEK293T or SH-SY5Y co-elute with the recombinant unfolded α-syn monomer in a Superdex 200 column (supplemental Fig. S4*A*). Furthermore, boiling of native α-syn from SH-SY5Y cells did not change its migration or apparent molecular weight in both native (supplemental Fig. S1*B*) and denaturing gels (data not shown), suggesting that α-syn produced in these cell lines is devoid of a stable structure and is monomeric. We also examined SDS-induced denaturation of both recombinant proteins and SH-SY5Y cell lysates (supplemental Fig. S1, *A* and *B*, respectively), and found that the negative charge added upon SDS binding significantly increases the mobility of the protein on native gels, making this method unsuitable to assess the effect of SDS-induced denaturation on α-syn migration.

To further characterize the oligomerization of α-syn, we used the oligomer specific ELISA developed by El-Agnaf *et al.* (55) (Fig. 6*A*). To test whether cellular factors present in the cell lysate could induce oligomerization of exogenous α-syn, recombinant α-syn monomer ("fresh") was also added to the cell lysates in a parallel experiment. Aggregated (aged) α-syn was added to the cell lysates as positive control. As shown in Fig. 6*B*, the signals from "endogenous" (*red bars*) and "exogenous" (*black bars*) α-syn were similar. Importantly, the signals obtained from endogenous α-syn and exogenous monomeric α-syn were on the same order of magnitude as those observed

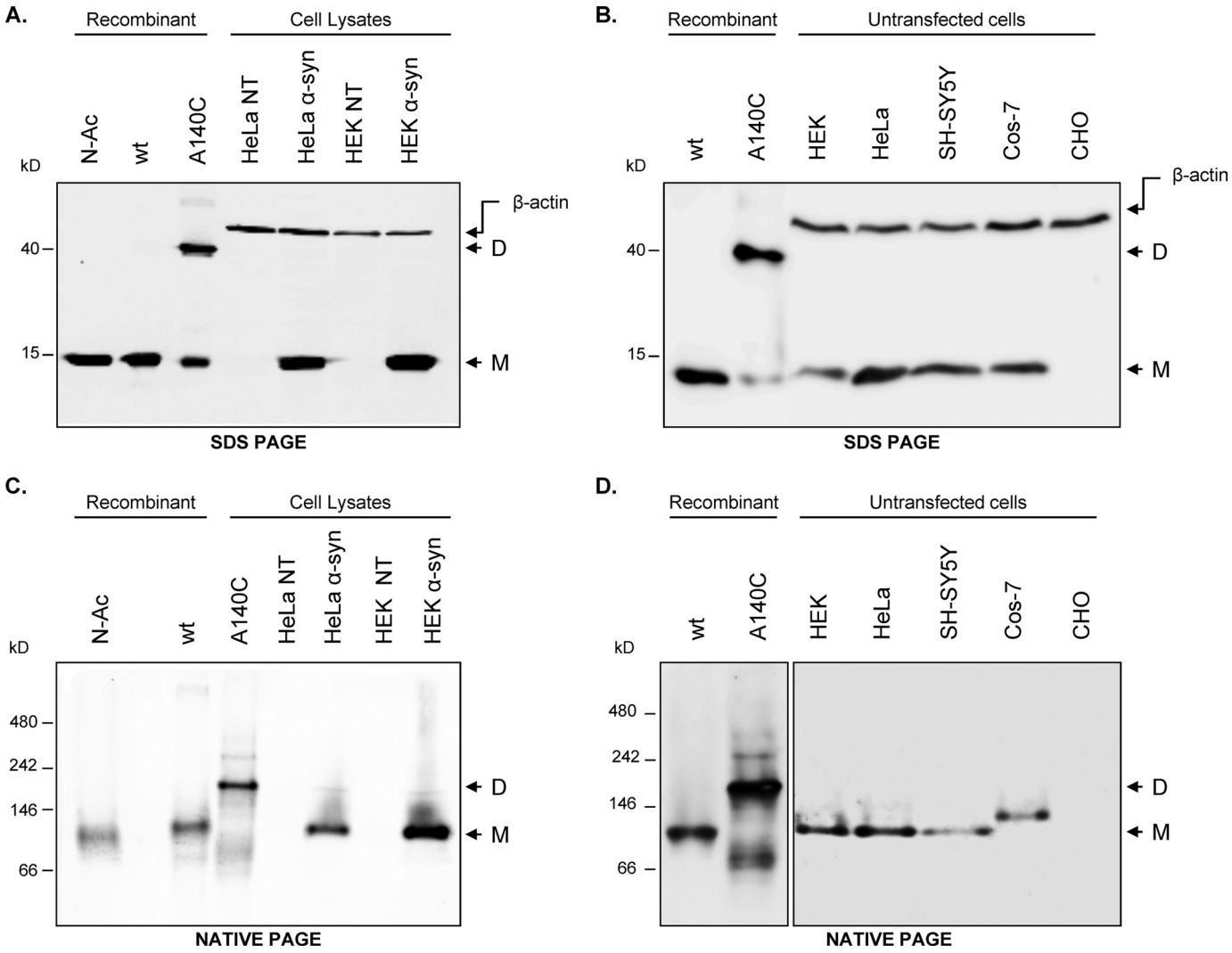

FIGURE 5. **Recombinant and native (endogenous and overexpressed) α-syn co-migrate as single monomeric species.** *A*, SDS-PAGE of cell lysate obtained from HEK293T and HeLa cells transiently transfected or not (control) with a plasmid encoding WT human α-syn. Both recombinant (*N-Ac* and *wt*) and exogenous α-syn co-migrate at 15 kDa. The blot was revealed by fluorescence scanned at lower exposure, allowing the detection of exogenous α-syn only. *B*, SDS-PAGE of five different mammalian cell lines screened for endogenous α-syn expression and revealed by enhanced chemiluminescence. Native endogenous α-syn from these cells when detectable co-migrates with recombinant purified α-syn at 15 kDa. *C* and *D*, same samples obtained in *A* and *B*, respectively, were resolved in 7.5% CN-PAGE and revealed as described ("Experimental Procedures"). As shown, exogenous α-syn WT (*C*) and native α-syn co-migrate as single band above 66 kDa on CN-PAGE. Endogenous α-syn from the COS-7 cell line migrates slightly slower than recombinant α-syn and below the recombinant dimers. We failed to detect α-syn in CHO cell lysate in both conditions. *N-Ac*, recombinant purified *N*-acetylated α-syn; *Wt*, control recombinant purified α-syn; *A140C*, control recombinant purified dimers; *M*, α-syn monomers; *D*, α-syn dimers.

when untransfected cells expressed only very low α-syn levels and remained significantly lower than when multimerized (Fig. 6*B*, aged, *white bars*) α-syn was added to the lysates. These results suggest that the higher intracellular α-syn concentrations resulting from transfection did not result in significant oligomerization of the protein. As expected, the oligomer-specific ELISA successfully detected the presence of the 46-kDa α-syn oligomer detected in the RBC sample prepared using the protocol from Bartels *et al.* (1) (supplemental Fig. S5*D*), further confirming the robustness of this assay to detect small amount of oligomers.

Protein Cross-linking in Cells—We reasoned that our inability to detect stable oligomeric forms of α-syn could be explained by the fact that such oligomers are highly dynamic and/or unstable. To test this hypothesis, we performed protein cross-linking using the cell-permeable cross-linker disuccinimidyl suberate (spacer arm, 11.4 Å) under the same conditions recently reported by Bartels *et al.* (1). When cells overexpressing human α-syn were treated with disuccinimidyl suberate, we observed the formation of multiple α-syn SDS-resistant species in denaturing PAGE, with the dimer being the predominant species co-migrating at the same position as our disulfide-linked A140C α-syn dimer (Fig. 7*A*). Interestingly, in addition to monomeric and dimeric α-syn, small amounts of higher molecular weight species corresponding to higher order assembly states were also observed. Given that the α-syn monomers and dimers migrate with an apparent molecular mass of 17 and 36 kDa, respectively it is not clear if the band observed at ~57 kDa corresponds to α-syn trimer or tetramer. We also performed the same cross-linking experiments on untransfected as well as on stably transfected SH-SY5Y neuroblastoma cells having an intermediate level of α-syn expression. On SDS-PAGE,

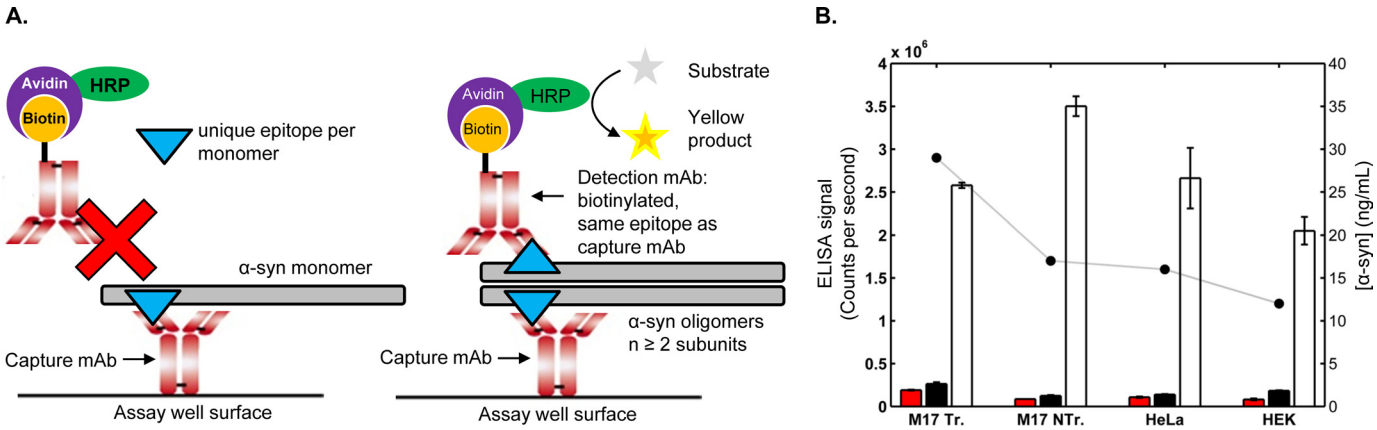

FIGURE 6. **Characterization of GST-α-syn and cell line-derived α-syn using an oligomer-specific ELISA.** *A,* schematic depiction of how the same monoclonal antibody in both "native" (*capture mAb*) and biotinylated (*detection mAb*) versions are used to specifically detect α-syn oligomers (*right scheme*). In this assay, monomers cannot be detected because the epitope is masked upon capture (*left scheme*). Adapted from El-Agnaf *et al.* (55). *B,* α-syn oligomer detection in cell lysates. The *left ordinate* axis shows the ELISA readings, and the *right ordinate* axis displays the total α-syn (monomers and oligomers) concentration, in nontransfected cell lysate, transfected cell lysate, cell lysate mixed with fresh α-syn, or cell lysate mixed with aged α-syn. The monomeric α-syn concentration (*black dots connected with a straight line*) were determined by a different sandwich ELISA. *M17 Tr.*, M17 cells transfected with WT human α-syn; *M17 NTr,* untransfected M17 cells. HeLa and HEK cells were untransfected.

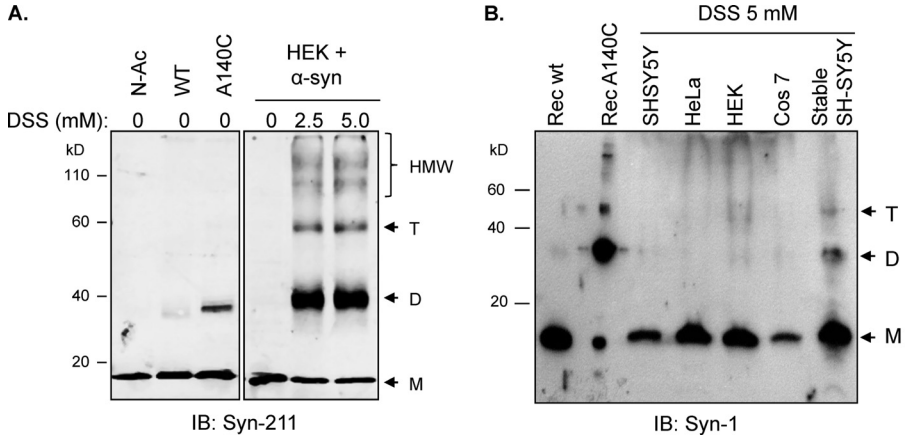

FIGURE 7. **In-cell and *in vitro* cross-linking of α-syn.** *A,* in-cell cross-linking of HEK293T cells overexpressing α-syn WT. Intact cells overexpressing α-syn were harvested, and cross-linking experiments were performed as described under "Experimental Procedures." Different oligomeric species of α-syn resistant to denaturing conditions are seen in the presence of 2.5 and 5 mM of cross-linker compared with nontreated cells. These higher molecular weight species are mainly dimers but also traces of trimers/tetramers, as well as high molecular weight oligomers (*HMW* indicated by a *bracket*). *B,* in-cell cross-linking of untransfected cells. Only the stable SH-SY5Y cells expressing low levels of α-syn showed distinct detectable higher molecular weight species of which the dimers remains the predominant species. Nontransfected cells in contrast showed very little formation of α-syn oligomers. *M,* monomer; *D,* dimer; *T*, trimer/tetramer; *IB*, immunoblot.

the monomer remained the predominant species, and we did not observe large amounts of cross-linked α-syn dimers in untransfected cells (Fig. 7*B*). In the case of the stable cell line, SH-SY5Y, we observed a small amount of dimers and trimers/tetramers, but the great majority of the protein was monomeric. The higher molecular weight species were also much less abundant in cross-linked samples of untransfected cells and even in the stably transfected SH-SY5Y cell line expressing moderate levels of α-syn (Fig. 7*B*, *right-most lane*). These observations are consistent with previous cross-linking studies (15, 56–59), which show predominantly α-syn dimers and a distribution of higher order oligomers.

Purification of Native α-syn from Human Erythrocytes—Altogether, our findings are more consistent with native α-syn in its free form being a predominantly unfolded and monomeric protein. In all our studies, we failed to detect stable oligomeric forms of native α-syn. Because much of the structural data presented by Bartels *et al.* (1) use RBC-derived human α-syn, we investigated the properties of α-syn from RBCs and compared its structure and migration properties with the monomeric and dimeric α-syn standards.

To characterize human α-syn from RBCs, we developed a purification protocol based on an immobilized metal affinity chromatography-based Hb depletion that relies on the affinity of the Hb heme prosthetic groups toward immobilized nickel ions, prior to α-syn purification by three consecutive chromatography steps (ion-exchange → HIC → SEC) as reported by Bartels *et al.* (1), see under "Experimental Procedures" and "supplemental material." Note that the second most abundant protein in RBCs, the 29-kDa carbonic anhydrase-1, is not depleted by this method. Hb depletion was then quantified by the Harboe spectrophotometric method (22). Five measurements were carried out, each in triplicate; the calculated remaining Hb in the depleted fraction was 4.7 ± 0.4%. By using Western blotting, we established that α-syn is present exclusively in the Hb-depleted fraction (supplemental Fig. S6*B*).

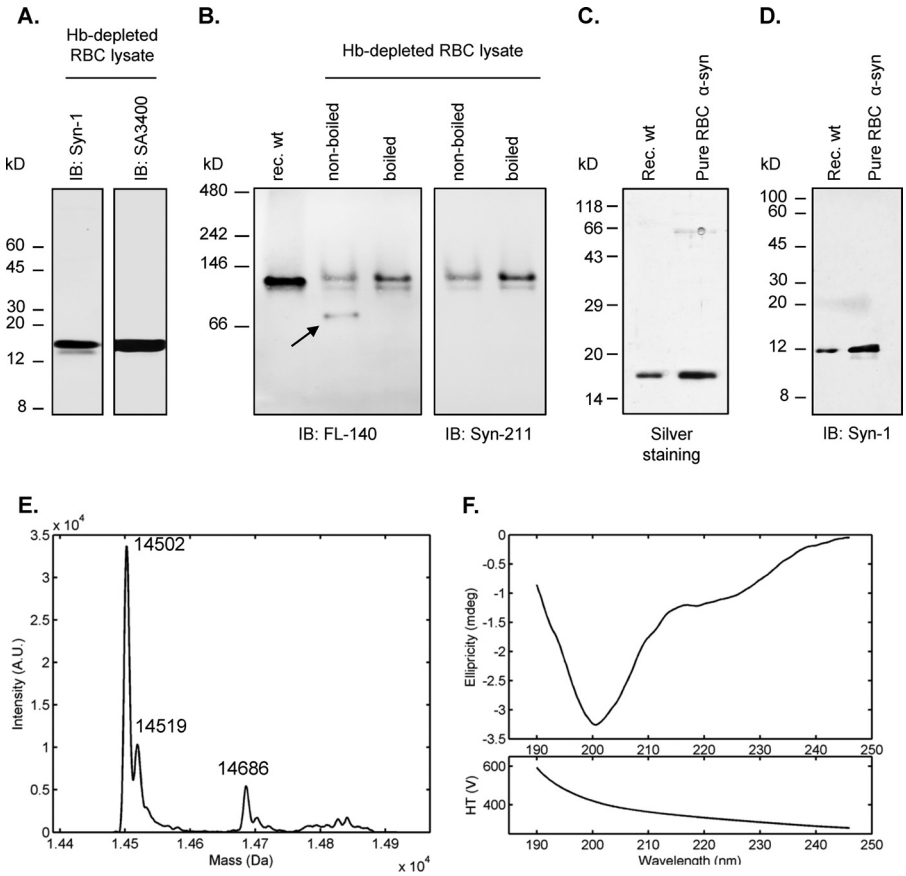

FIGURE 8. **Characterization of RBC-derived α-syn.** *A,* SDS-PAGE/Western blots of RBC-derived α-syn after Hb depletion, probed with two different primary antibodies as indicated *above* the blots. *B,* CN-PAGE analysis of 100 ng of RBC α-syn from an Hb-depleted lysate with or without heat-induced denaturation. The FL-140 (1:500) and SA3400 (1:2000) primary antibodies were used. Revelation was performed as in *A*. Boiled samples were heated at 100 °C for 10 min before loading in the sample wells. The *arrow* indicates a heat-labile, C-terminally truncated form of α-syn. *C,* characterization of the purified RBC-derived α-syn by SDS-PAGE/silver staining. *1st lane,* recombinant WT human α-syn control (20 ng). *2nd lane,* purified RBC α-syn (4 μl). *D,* SDS-PAGE/Western blot of the purified RBC-derived α-syn. 20 ng of recombinant α-syn were loaded as a control. Western blotting was done as in *A*. *E,* deconvoluted ESI-MS spectrum of purified RBC α-syn, ~100 ng of purified RBC-derived α-syn were loaded on a Poroshell 300SB C_3 column and eluted with increasing concentration of acetonitrile, 0.1% formic acid. The eluate was analyzed by an LTQ ion trap mass spectrometer. Charge state deconvolution was done using MagTran. *F,* CD spectroscopy (1-mm cell) of pure RBC α-syn after its buffer had been exchanged for 20 mM sodium phosphate, pH 7.4. *IB*, immunoblot.

Probing the Hb-depleted lysate with different primary antibodies confirmed the predominance of the full-length protein (Fig. 8*A*) in addition to a small amount of a truncated form of the protein. We then assessed the oligomeric state of RBC-derived α-syn in the Hb-depleted lysate by CN-PAGE and Western blot. α-Syn from RBCs co-migrated with recombinantly expressed WT human α-syn, and denaturing it by heating did not influence its migration in native gels (Fig. 8*B*), thus suggesting that native α-syn from RBCs exists as a heat-stable monomeric state with an extended conformation, very similarly to the bacterially expressed standard. Note that in the Hb-depleted lysate, RBC-derived α-syn migrated as three species, the lowest of which is heat-labile, a property likely that can be explained by the absence of the C-terminal domain in this species, as revealed by Western blotting with the C-terminal-specific antibody Syn-211 (Fig. 8*B*, *right panel*). Further studies are underway to determine whether the additional species correspond to C-terminal fragments due to proteolysis or correspond to alternative splicing isoforms of α-syn as suggested by Bartels *et al.* (1). The remaining Hbs, as well as carbonic anhydrase-1, were then removed in the anion-exchange chromatography step (supplemental Fig. S6*C*), and the fractions containing α-syn were subjected to further purification by HIC and size-exclusion chromatography (see supplemental material).

Although this protocol allowed us to obtain highly pure material, the yield was too low to allow light scattering and analytical ultracentrifugation analyses. However, we had sufficient material to carry out mass spectrometry and CD spectroscopy analyses. SDS-PAGE/silver staining of pooled gel-filtration fractions after concentration showed a purity of > 95% (Fig. 8*C*), a result confirmed by Western blotting (Fig. 8*D*). Electrospray ionization-mass spectrometric analysis (Fig. 8*E*) of purified RBC showed a main peak at 14,502 Da, a mass that exactly matches that of a single acetylation of human α-syn. The mass at 14,519 Da is consistent with a single methionine oxidation (theoretical mass, 14,518 Da), whereas the peak at 14,686 Da corresponds to the presence of slight amounts of covalently modified α-syn by 4-(2-aminoethyl)benzenesulfonyl fluoride (theoretical mass, 14,685 Da), a commonly used protease inhibitor which is present in the mixture we used for lysis. The CD spectrum of RBC-derived α-syn exhibited a main minimum around 200 nm, consistent with a predominantly disordered conformation (Fig. 8*F*), a finding that is consistent with all other analyses carried out in this study, as well as with pre-

viously published work on α-syn (6). The presence of a shoulder at ~218 nm is characteristic of α-syn, although it is more pronounced here. We believe that this signal comes from the presence of some α-syn aggregates resulting from the extensive concentration steps required to obtain samples that are suitable for CD measurements. We stress that care should be taken to prevent the dynode voltage of the CD from saturating in the 190–205 nm wavelength region, as this leads to masking of random coil signals and the appearance of false-positive CD signals.

We also attempted to purify human RBC α-syn according to the protocol published by Bartels and co-workers (61). This experiment was performed on a blood sample from a different donor. From the three suggested bulk purification techniques (after pre-purification by differential ammonium sulfate precipitations, as described (61)), we chose to perform ion-exchange chromatography followed by gel filtration, because Hb, the most prevalent contaminant, should not bind the anion-exchange column under the conditions described. Purity assessment by SDS-PAGE/silver staining (supplemental Fig. S5*C*) showed the presence of many contaminants, and subsequent repurification using HIC failed to produce pure samples in sufficient amount and purity for conducting detailed biophysical studies. Interestingly, SDS-PAGE/Western blotting analysis of total RBC lysates and anion-exchange chromatography fractions revealed the presence of an additional α-syn-immunoreactive band migrating at ~46 kDa, in addition to the α-syn monomer band at ~14 kDa (supplemental Fig. S5*A*). The specificity of this higher molecular band to human α-syn was verified using three different primary antibodies against human α-syn and by immunoprecipitation (supplemental Fig. S5*A* and *B*). Notably, this high molecular weight species is resistant to boiling, SDS, and reducing agents that are present in the sample loading buffer, suggesting it may consist of a cross-linked α-syn oligomer or α-syn cross-linked to another protein. Proteolytic digestion followed by tandem mass spectrometry analyses established the presence of α-syn in the ~46-kDa complex, where six unique peptides exclusive to human α-syn were identified (supplemental Fig. S5, *E* and *F*), thus further confirming the immunoblot data. It is important that one does not confuse this ~46-kDa band with the putative tetramer reported by Bartels *et al.* (1) because they did not detect any SDS-stable oligomers in their samples of α-syn purified from RBCs.

Previous studies have suggested that native α-syn is subjected to N-terminal acetylation (35, 36). Using tandem mass spectrometry of GluC-digested samples, we now confirm that RBC α-syn is quantitatively acetylated at its N terminus, thus establishing that this modification is ubiquitous and not restricted to α-syn in the brain (35, 36).[3]

Expression of α-syn as GST Fusion Followed by Cleavage Results in Release of Unfolded Monomeric α-syn—Recently, Wang *et al.* (2) reported that expression of α-syn as a GST fusion protein in *E. coli* followed by removal of GST results in α-syn that is tetrameric and rich in α-helical structure. Therefore, we attempted to replicate these findings in our laboratory. In addition, similar studies were carried out independently by El-Agnaf *et al.* (55). We used cleavable GST-α-syn constructs based on an N-terminal fusion of GST to α-syn. The proteins were purified, and the GST tag was then removed under nondenaturing conditions as described above. We observed that α-syn after removal of the GST exists predominantly as an unfolded monomer. Interestingly, we observed that the GST-α-syn fusion protein exists as a mixture of oligomers as discerned by size-exclusion chromatography and light scattering (supplemental Fig. S7). We speculated that this oligomerization is driven by GST itself and not α-syn, because the GST used in pGEX plasmids, originally isolated from the parasite *Schistosoma japonicum* (62), naturally exists as a dimer (see Protein Data Bank entry 1GNE (63)), as do GST homologs from various species (64, 65). In support of this hypothesis, we observed very fast kinetics for the proteolysis of the GST tag by thrombin, suggesting the cleavage site is very accessible, a situation much more likely when the α-syn domain of the fusion protein is unfolded and not participating in close intermolecular interactions. Furthermore, the type of the observed GST-α-syn oligomers depended upon the length of treatment with reducing agents (short treatments produced a mixture of tetramers and octamers, longer ~20-min treatments with 10 mM DTT produced a mix of dimers and pentamers, whereas under nonreducing conditions the protein eluted in the void volume of Superdex 200 and showed a molar mass of >1 MDa). Upon cleavage of GST, α-syn elutes at a position similar to that of the unfolded monomer. Cleavage and release of α-syn was quantitative as seen by SDS-PAGE (Fig. 9*A*). Furthermore, on CN-PAGE, the cleaved GST-α-syn migrated slightly slower than recombinant WT α-syn, most probably due to the 9 additional residues remaining after cleavage and the presence of two positively charged residues within this sequence (Fig. 9*B*). Boiling the sample did not affect the migration of the cleaved GST-α-syn under nondenaturing conditions. If α-syn is responsible for the oligomerization of the uncleaved fusion protein, individual monomers should be close enough to be cross-linked by BS^3, a water-soluble cross-linking agent with a 11.4-Å spacer length. The cross-linked α-syn oligomers should then be detectable on SDS-polyacrylamide gels. To determine whether α-syn oligomerization could be already present in the GST-α-syn fusion protein, we treated the protein (1 mg/ml) with 5 mM BS^3 for 15 min. After blocking unreacted BS^3 with 50 mM Tris, pH 7.6, the GST tag was released by treatment with thrombin (RT, 1 h). The different species were then resolved on SDS-PAGE and probed by Western blot against α-syn (Fig. 9*C*). GST-α-syn was reduced with 10 mM DTT prior to cross-linking, because we observed that nonreduced GST forms high molecular weight species as discussed above. Cross-linking of the fusion protein (without thrombin treatment, Fig. 9*C*, *2nd lane*) stabilized several oligomeric species (bands above the 60-kDa mark), including dimers and tetramers (although the tetramer band is not well resolved). When BS^3-treated GST-α-syn was further incubated with thrombin to cleave off the GST tag (Fig. 9*C*, *4th lane*), we did not observe any low-order oligomeric α-syn species such as dimer, trimer, or tetramer but instead high molecular weight complexes migrating at >100 kDa that may correspond to uncleaved cross-linked GST-α-syn (in which the

[3] H. A. Lashuel, unpublished results.

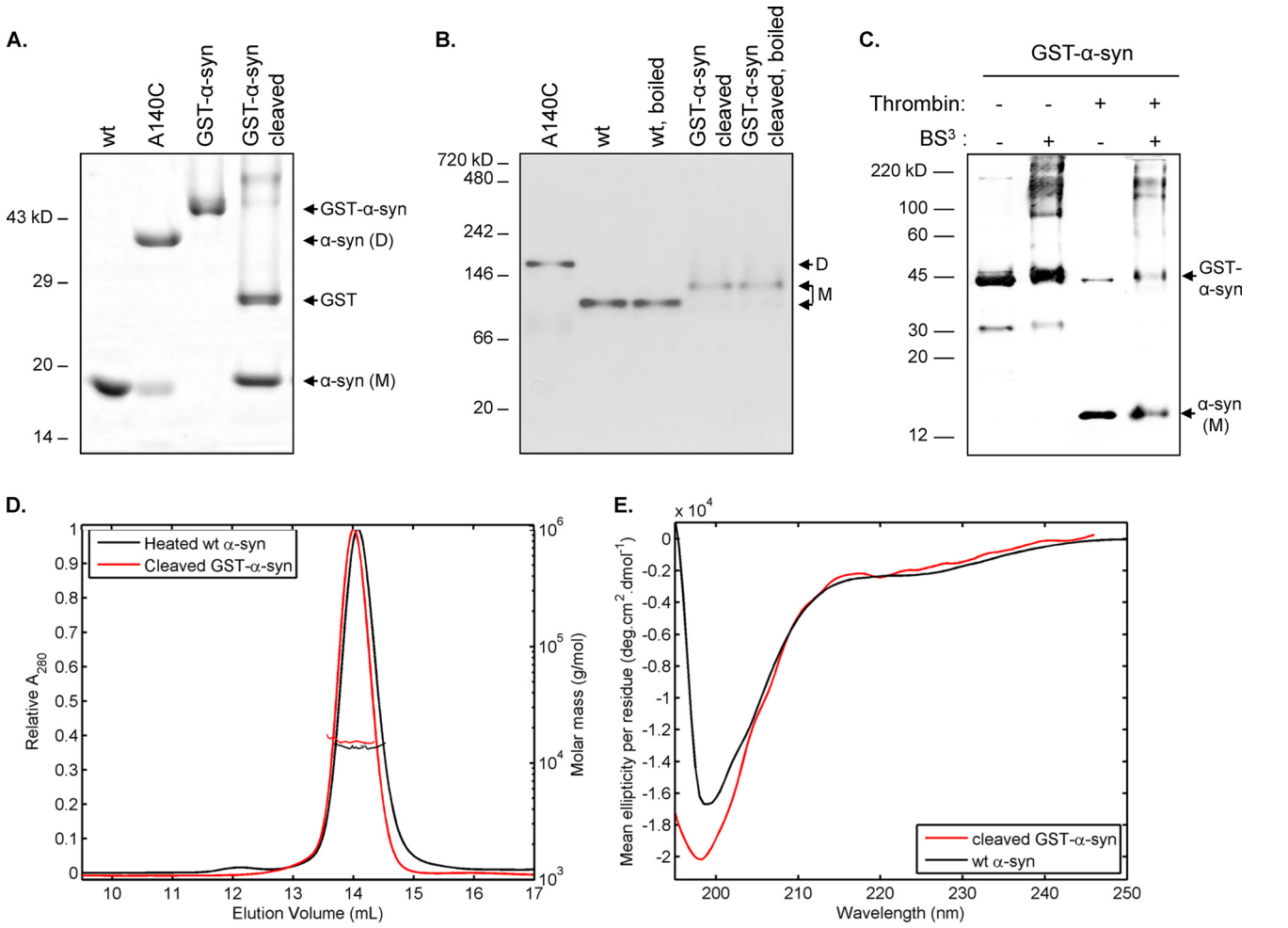

FIGURE 9. **Recombinant purified GST-α-syn remains an unfolded monomer after removal of the GST tag.** *A,* SDS-PAGE/Coomassie Blue staining of GST-α-syn cleavage by thrombin. 2 μg of proteins were loaded in each lane. Removal of the tag was nearly quantitative after 1 h at RT. *B,* CN-PAGE analysis of purified α-syn after removal of the GST tag. Purification was performed entirely under nondenaturing conditions as described under "Experimental Procedures." The lower mobility of cleaved GST-α-syn is attributable to both the presence of 9 additional residues at its N terminus and the fact that two of them are positively charged, hence shifting the net charge of the protein. Boiling (100 °C, 10 min) prior to electrophoresis did not change its mobility. *C,* cross-linking study of GST-α-syn. 1 mg/ml of reduced (10 mM DTT) fusion protein in 20 mM phosphate buffer, pH 7.6, was treated with 5 mM BS^3 for 15 min at RT (*2nd* and *4th lanes*) or simply incubated in phosphate buffer as negative control (*1st* and *3rd lanes*). Then thrombin (10 units/mg of GST-α-syn) was applied to remove the GST tag (*3rd* and *4th lanes*). Proteins were resolved on 15% SDS-polyacrylamide gels and revealed by Western blotting (Syn-1, 1:2000, overnight, 4 °C). *D,* analytical gel filtration/light scattering analysis of purified cleaved GST-α-syn. 100 μl of protein samples at 20 μM were injected and analyzed as indicated under "Experimental Procedures." Cleaved GST-α-syn and denatured recombinant WT α-syn co-elute and are monomeric. *E,* CD spectroscopy was performed at a protein concentration of 5 μM. The spectra shown are averages of 10 runs. *M,* α-syn monomers; *D,* α-syn dimers.

thrombin cleavage site had been made inaccessible due to cross-linking). We then performed biophysical studies on the protein after the GST tag was removed. After GST removal, α-syn eluted at the same position as denatured WT α-syn on gel-filtration column, and measurement of its molecular mass by static light-scattering showed that the protein exists as a monomer (Fig. 9*D*), which was also shown to be unfolded by CD spectroscopy (Fig. 9*E*).

Similar findings were observed independently by El-Agnaf *et al.* (55) using a different GST-α-syn construct and purification protocol (described under "Experimental Procedures"). An oligomer-specific ELISA was also employed (see scheme on Fig. 6*A*), which successfully recognized uncleaved GST-α-syn as well as aggregated (aged) α-syn (positive control) but not recombinant denatured α-syn nor GST alone (negative controls) (Fig. 10). These data are consistent with our observation that the GST-α-syn fusion protein is oligomerized before removal of the GST tag; however, upon treatment with thrombin, the cleaved α-syn co-migrated with recombinant α-syn monomer on CN-PAGE (data not shown), thus further supporting the observation that GST is driving the self-association of the construct.

Altogether, these results further confirm our findings that α-syn expressed in *E. coli* is monomeric and unfolded and suggest that the GST tag does not stabilize any oligomeric state of α-syn. The results are consistent with the long standing view that native state of α-syn, at least on its own, exists predominantly in a monomeric disordered conformation.

DISCUSSION

Since its discovery and isolation from human brains, it has been widely accepted that α-syn exists as an intrinsically disordered monomeric protein (6, 7). However, a recent study by Bartels *et al.* (1) suggested that physiological α-syn exists as a

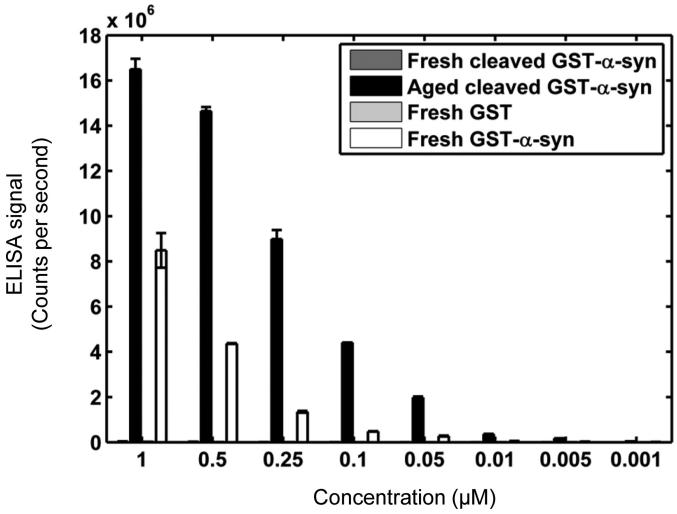

FIGURE 10. **Detection of α-syn oligomers *in vitro* using an ELISA-based assay.** Serial dilution shows the specificity of the ELISA to α-syn oligomers. Only aged (aggregated) and cleaved GST-α-syn and freshly prepared non-cleaved α-syn fused to GST were detectable in a concentration-dependent manner. The sensitivity of the assay was below 5 nM.

stable tetramer that is rich in α-helical structure and resistant to amyloid formation. Another study by Wang *et al.* (2) suggested that α-syn produced in *E. coli* exists as a stable α-helical rich tetramer in the absence of lipid bilayers or micelles. Given the significant implications of these findings and the fact that these studies focused primarily on α-syn derived from *E. coli*, cell lines, and RBCs, we initially sought to reinvestigate the native state of α-syn produced in *E. coli* and then extended our studies to assess the oligomeric state of α-syn in various mammalian cell lines as well as in mouse, rat, and human brains. As such, we investigated the oligomeric state of α-syn in the following: 1) transgenic mice expressing human α-syn; 2) rat brains infected by AAVs encoding WT human α-syn; and 3) human brain (frontal cortex) homogenates from control, AD, and LBD cases. In all of these studies, protein extraction was carried out at all times under nondenaturing conditions.

To allow accurate assessment of the oligomeric state of native α-syn and comparison of α-syn derived from different sources, we generated a series of α-syn standards of well defined conformational and oligomeric states. These included the following: 1) unfolded monomeric WT α-syn; 2) disulfide-linked α-syn dimer (A140C mutation); and 3) α-syn specifically acetylated at the N terminus. To ensure reproducibility and to validate results across different laboratories, these standards were provided to four independent research groups, which are part of this study, for use as controls in studies aimed at assessing the oligomeric state of native α-syn from different sources. In total, seven independent groups participated in the work presented here.

Together, our findings show the following: 1) α-syn expressed in *E. coli* and purified under denaturing or nondenaturing conditions is monomeric and adopts disordered conformations; 2) the unfolded α-syn monomer co-elutes and co-migrates in native gels and SEC with native α-syn (endogenous or overexpressed) from mammalian cells or isolated under nondenaturing conditions, from mouse, rat, and human brains; 3) by using an oligomer-specific ELISA (55), we failed to detect α-syn oligomers in mammalian cells and cells expressing α-syn at different levels (Fig. 6*B*); and 4) boiling the native or recombinant unfolded monomer does not affect their migration at an apparent molecular mass slightly above 66 kDa in clear native gels. Interestingly, the disulfide-linked dimer (A140C) migrated slower, whereas phosphorylated forms of α-syn (Ser(P)-87, and Ser(P)-129) migrated faster than the unfolded recombinant α-syn or native α-syn. These results suggest that the use of native gels, although not accurate predictors of molecular weight of proteins, can still differentiate different oligomeric or modified forms of α-syn. Finally, the co-migration of unfolded and native α-syn suggests that both of these proteins exist as unfolded monomers (6).

Recombinant α-syn Produced in E. coli Exist as Disordered Monomers—Our results demonstrating that α-syn produced in *E. coli* is monomeric and unfolded are consistent with previous studies by Lansbury and co-workers (6), who also demonstrated that the 66-kDa band in native gels corresponds to unfolded monomeric α-syn. When the migration of α-syn in Native-PAGE was assessed at different acrylamide concentrations and the molecular weight was extrapolated from the Ferguson plots (66), they estimated the α-syn native molecular mass to be 20 ± 3 kDa. Furthermore, sucrose gradient ultracentrifugation studies by the same group showed that recombinant α-syn, purified under native or denaturing conditions, sediments more slowly than globular proteins of similar size, consistent with an elongated shape and absence of secondary structure as assessed by CD and Fourier transform infrared spectroscopy. Moreover, the measured sedimentation coefficient of 1.7 S, is consistent with a smaller globular protein of ~10 kDa. These results have been confirmed by many other independent groups on α-syn purified under native or denaturing conditions. In particular, CD measurements have always shown that free soluble α-syn is a random coil (43, 44). NMR studies also support the natively disordered character of α-syn; first, $^{1}H/^{15}N$-HSQC spectra show a narrow dispersion of chemical shifts (23, 67). Other lines of evidence based on NMR also support an unstructured nature for α-syn; chemical shift values for $^{13}C^{\alpha}$, $^{13}C^{\beta}$, and $^{1}H^{\alpha}$ can be combined into a single per residue score, which is sensitive to local secondary structure propensity score (68). Finally, data from paramagnetic relaxation enhancement is consistent with a disordered collapsed structure for monomeric α-syn where the N- and C-terminal regions participate in transient intramolecular contacts (44, 46, 69).

Given that the protein used in the studies Wang *et al.* (2) was expressed as a GST fusion protein, we wondered if the presence of GST, which is known to oligomerize, could favor or facilitate the folding and oligomerization of α-syn. To test this hypothesis, we assessed the oligomeric state of a α-syn fused to GST (GST-α-syn) prior to and after the removal of the GST tag. We observed that the GST-α-syn fusion protein exists as an oligomer using two different constructs and independent techniques; one is static light scattering, which showed a small amount of tetramers and a predominance of octamers, and the other is an oligomer-specific ELISA developed by El-Agnaf *et al.* (55). Such oligomers are most likely initiated by the dimerization of the GST domain, which is known to occur in

nature (63–65), but it remains possible that α-syn drives the formation of the higher order oligomers we observed by light scattering. However, here we demonstrated that the expression of α-syn as a GST fusion does not influence its quaternary structure and conformational states after removal of GST, *i.e.* the protein exists as an unfolded monomer. The presence of the additional nine amino acids (sequence, GSRRASVGS) in α-syn upon cleavage from GST-α-syn does not appear to influence its conformation of an oligomeric state. These findings were established unambiguously through the use of static light scattering and by the observation that once the GST tag is cleaved, heating does not affect the migration of the protein on Native-PAGE, below the dimeric α-syn standard (but above the recombinant WT monomer due to the 10-residue segment remaining after GST removal).

When studying α-syn extracted under nondenaturing conditions from mouse, rat, and human brain homogenates using CN-PAGE, the protein co-migrated with recombinant monomeric α-syn, suggesting a similar assembly state for brain-derived α-syn. The same studies were conducted on cell lysates prepared from both untransfected and transfected cell lines and both showed similar results. Using a cell-permeable cross-linker, we then tried to stabilize putative endogenous α-syn oligomers. In transiently transfected HEK293T cells that express very high levels of α-syn, we detected dimers as the main α-syn oligomeric species. The cross-linking pattern we observed in transfected HEK293T cells is consistent with the majority of cross-linking studies of native and recombinant α-syn reported in the literature. The predominance of dimers within low order oligomers is seen under various conditions, such as oxidative stress-induced dityrosine cross-linking (15, 70, 71), advanced glycation end product-mediated cross-linking (59), as well as metal ion-induced (57) and Coomassie Brilliant Blue-induced cross-linking (56).

Given that our Native-PAGE data show that α-syn from cell lines migrates as a single species, the distribution of cross-linked α-syn species in transfected cells or high concentration samples *in vitro* may reflect a cross-linking artifact, resulting in the observation of diffusion-limited cross-linking reactions of originally separate monomers. Alternatively, our data may also reflect the fact that the dimer could be the prevalent α-syn species in cells, suggesting it could serve as the basic building block for a very complex further assembly mechanism. Because we did not observe such dimers on Native-PAGE (without using any cross-linking agent), it is likely that if present under physiological conditions naturally occurring dimers are highly dynamic, with an equilibrium largely in favor of the monomer.

Overall, our results combined with extensive studies performed by other groups (6, 50) as well as ours (44) have shown that monomeric unfolded α-syn has a Stokes radius of 29–34 Å, which corresponds to an effective molecular mass of ~58 kDa for a typical globular protein. The fact that the measured Stokes radii at physiological pH values are smaller than expected for a fully extended random coil was explained by the presence of transient intramolecular interactions between the N- and C-terminal regions of α-syn (72). Thus, the fact that α-syn migrates with an apparent molecular mass slightly above 66-kDa in native gels and SEC is likely the result of its tendency to adopt extended conformations and not because it exists in an oligomeric form, *e.g.* tetramer. This hypothesis is supported by the facts that boiling of native α-syn from cells and brain tissue does not change its migration and co-elution with native α-syn from mammalian cells and mouse brain.

The use of well characterized α-syn standards of different sizes and charge states allowed us to assess and test the limitations of native gels and SEC for assessing the distribution of native α-syn in complex mixtures. Although the presence of the Coomassie dye in Blue Native gels compensates for the effect of charge, estimation of the protein's molecular weight still relies on globular standards. In our study, using both Blue and Clear Native-PAGE, we confirmed that denatured monomeric α-syn (as assessed by CD and static light scattering) migrates abnormally slowly, as expected from the extended shape conferred by the disordered state of α-syn. Most importantly, we reproducibly showed that native α-syn from brain and cell lines co-migrate with denatured α-syn samples, thus strongly supporting the intrinsically disordered α-syn model. The migration of α-syn did not change under denaturing conditions (boiling).

Finally, we used an optimized purification protocol to assess the oligomeric state of α-syn in RBCs (see "Experimental Procedures" and supplemental figures). Using this protocol, we obtained native α-syn with >95% purity as determined by SDS-PAGE and mass spectrometry (Fig. 8, *C* and *D*). The CD results shown in Fig. 8*E* demonstrate that native α-syn from RBC is predominantly unstructured. Using Native-PAGE, we established that α-syn from RBCs migrates at the same position as the recombinant unfolded α-syn, and this migration is not affected by heat denaturation, consistent with the thermostable monomeric state and similar to what has been reported for the recombinant protein (6). Consistent with the observation made by Bartels *et al.* (1), we observed additional bands of lower mass (see Fig. 8, *A* and *B*, and supplemental Fig. S6*C*), which could correspond to alternative splicing isoforms or could be a result of proteolytic processing of α-syn. In our case, these bands were not present in significant amounts after the final step of purification (Fig. 8, *C* and *D*).

In a blood sample from a different donor that was purified using the protocol developed by Bartels *et al.* (1), we observed a heat- and SDS-stable α-syn-positive band migrating at ~46 kDa. However, it is worth noting that Bartels *et al.* (1) did not report the detection of any SDS-resistant α-syn oligomers in their denaturing gels. Using Western blotting, oligomer-specific ELISA, immunoprecipitation, and mass spectrometry, we confirmed that this additional band corresponds to an oligomeric form of α-syn. Although not enough material was available to identify other potential members of this complex (if any) with confidence, the fact that it is resistant to SDS, heating, and reducing agents already suggests it may consist of a cross-linked α-syn oligomer or α-syn cross-linked to another protein. A more systematic study on a larger number of blood donors is required to determine whether this ~46-kDa complex could have been an artifact or is indeed present in the blood of some donors but not others.

In conclusion, our findings validate the widely accepted model of α-syn existing physiologically as a natively unfolded monomer, but it does not rule out the possibility that α-syn

could exist in a folded conformation or as a dynamic oligomer upon interacting with other proteins, protein complexes, and/or biological membranes. Although *in vitro* studies consistently show that α-syn adopts α-helical conformations upon binding to synthetic vesicles, very little is known about the conformation and oligomeric state of membrane-associated α-syn in neurons. Based on the existing data, we believe that therapeutic strategies aimed at stabilizing the monomeric form of α-syn, lowering its levels, and/or inhibiting the process of α-syn fibril formation (73) remain viable strategies for the treatment of Parkinson disease and related disorders. Finally, our work stresses the critical importance of using proper standards and assays to study the oligomeric state of proteins with an unfolded character.

Acknowledgments—We are grateful to John Perrin, Nathalie Jordan, Viviane Padrun, Fabienne Pidoux, and Philippe Colin for their outstanding technical support, as well as Dr. Abid Oueslati and Mirva Hejjaoui for helpful comments and discussions. We express our gratitude to Prof. Jean-Daniel Tissot from the Service Régional Vaudois de Transfusion Sanguine for assistance with RBC collection, lysis, and Hb depletion. We also thank Diego Chiappe, Romain Hamelin, and Dr. Marc Moniatte (Proteomics Core Facility, EPFL, Lausanne, Switzerland) for mass spectrometric analysis of RBC-derived α-syn. We are also grateful to Dr. Julia George (University of Illinois, Urbana-Champaign) and Dr. Hyangshuk Rhim (The Catholic University College of Medicine, Seoul, Korea) for kindly providing us the pGEX-2TK-α-syn and pGEX-4T1-α-syn plasmids, respectively. We also thank Dr. Michael K. Lee (Dept. of Neuroscience, University of Minnesota, Minneapolis) for providing the A53T α-syn transgenic mice. We also thank Jonathan Lovas for generating the A140C α-syn construct.

REFERENCES

1. Bartels, T., Choi, J. G., and Selkoe, D. J. (2011) α-Synuclein occurs physiologically as a helically folded tetramer that resists aggregation. *Nature* **477,** 107–110
2. Wang, W., Perovic, I., Chittuluru, J., Kaganovich, A., Nguyen, L. T., Liao, J., Auclair, J. R., Johnson, D., Landeru, A., Simorellis, A. K., Ju, S., Cookson, M. R., Asturias, F. J., Agar, J. N., Webb, B. N., Kang, C., Ringe, D., Petsko, G. A., Pochapsky, T. C., and Hoang, Q. Q. (2011) A soluble α-synuclein construct forms a dynamic tetramer. *Proc. Natl. Acad. Sci.* **108,** 17797–17802
3. Spillantini, M. G., Crowther, R. A., Jakes, R., Hasegawa, M., and Goedert, M. (1998) α-Synuclein in filamentous inclusions of Lewy bodies from Parkinson disease and dementia with Lewy bodies. *Proc. Natl. Acad. Sci.* **95,** 6469–6473
4. Baba, M., Nakajo, S., Tu, P. H., Tomita, T., Nakaya, K., Lee, V. M., Trojanowski, J. Q., and Iwatsubo, T. (1998) Aggregation of α-synuclein in Lewy bodies of sporadic Parkinson disease and dementia with Lewy bodies. *Am. J. Pathol.* **152,** 879–884
5. Cookson, M. R. (2009) α-Synuclein and neuronal cell death. *Mol. Neurodegener.* **4,** 9
6. Weinreb, P. H., Zhen, W., Poon, A. W., Conway, K. A., and Lansbury, P. T., Jr. (1996) NACP, a protein implicated in Alzheimer's disease and learning, is natively unfolded. *Biochemistry* **35,** 13709–13715
7. Conway, K. A., Harper, J. D., and Lansbury, P. T. (1998) Accelerated *in vitro* fibril formation by a mutant α-synuclein linked to early-onset Parkinson disease. *Nat. Med.* **4,** 1318–1320
8. Chartier-Harlin, M. C., Kachergus, J., Roumier, C., Mouroux, V., Douay, X., Lincoln, S., Levecque, C., Larvor, L., Andrieux, J., Hulihan, M., Waucquier, N., Defebvre, L., Amouyel, P., Farrer, M., and Destée, A. (2004) α-Synuclein locus duplication as a cause of familial Parkinson disease. *Lancet* **364,** 1167–1169
9. Singleton, A. B., Farrer, M., Johnson, J., Singleton, A., Hague, S., Kachergus, J., Hulihan, M., Peuralinna, T., Dutra, A., Nussbaum, R., Lincoln, S., Crawley, A., Hanson, M., Maraganore, D., Adler, C., Cookson, M. R., Muenter, M., Baptista, M., Miller, D., Blancato, J., Hardy, J., and Gwinn-Hardy, K. (2003) α-Synuclein locus triplication causes Parkinson disease. *Science* **302,** 841
10. Polymeropoulos, M. H., Lavedan, C., Leroy, E., Ide, S. E., Dehejia, A., Dutra, A., Pike, B., Root, H., Rubenstein, J., Boyer, R., Stenroos, E. S., Chandrasekharappa, S., Athanassiadou, A., Papapetropoulos, T., Johnson, W. G., Lazzarini, A. M., Duvoisin, R. C., Di Iorio, G., Golbe, L. I., and Nussbaum, R. L. (1997) Mutation in the α-synuclein gene identified in families with Parkinson disease. *Science* **276,** 2045–2047
11. Zarranz, J. J., Alegre, J., Gómez-Esteban, J. C., Lezcano, E., Ros, R., Ampuero, I., Vidal, L., Hoenicka, J., Rodriguez, O., Atarés, B., Llorens, V., Gomez Tortosa, E., del Ser, T., Muñoz, D. G., and de Yebenes, J. G. (2004) The new mutation, E46K, of α-synuclein causes Parkinson and Lewy body dementia. *Ann. Neurol.* **55,** 164–173
12. Muñoz, E., Oliva, R., Obach, V., Martí, M. J., Pastor, P., Ballesta, F., and Tolosa, E. (1997) Identification of Spanish familial Parkinson disease and screening for the A53T mutation of the α-synuclein gene in early onset patients. *Neurosci. Lett.* **235,** 57–60
13. Duda, J. E., Giasson, B. I., Chen, Q., Gur, T. L., Hurtig, H. I., Stern, M. B., Gollomp, S. M., Ischiropoulos, H., Lee, V. M., and Trojanowski, J. Q. (2000) Widespread nitration of pathological inclusions in neurodegenerative synucleinopathies. *Am. J. Pathol.* **157,** 1439–1445
14. Giasson, B. I., Duda, J. E., Murray, I. V., Chen, Q., Souza, J. M., Hurtig, H. I., Ischiropoulos, H., Trojanowski, J. Q., and Lee, V. M. (2000) Oxidative damage linked to neurodegeneration by selective α-synuclein nitration in synucleinopathy lesions. *Science* **290,** 985–989
15. Souza, J. M., Giasson, B. I., Chen, Q., Lee, V. M., and Ischiropoulos, H. (2000) Dityrosine cross-linking promotes formation of stable α-synuclein polymers. Implication of nitrative and oxidative stress in the pathogenesis of neurodegenerative synucleinopathies. *J. Biol. Chem.* **275,** 18344–18349
16. Yamin, G., Uversky, V. N., and Fink, A. L. (2003) Nitration inhibits fibrillation of human α-synuclein *in vitro* by formation of soluble oligomers. *FEBS Lett.* **542,** 147–152
17. Binolfi, A., Rasia, R. M., Bertoncini, C. W., Ceolin, M., Zweckstetter, M., Griesinger, C., Jovin, T. M., and Fernández, C. O. (2006) Interaction of α-synuclein with divalent metal ions reveals key differences: a link between structure, binding specificity, and fibrillation enhancement. *J. Am. Chem. Soc.* **128,** 9893–9901
18. Santner, A., and Uversky, V. N. (2010) Metalloproteomics and metal toxicology of α-synuclein. *Metallomics* **2,** 378–392
19. Lücking, C. B., and Brice, A. (2000) α-Synuclein and Parkinson disease. *Cell. Mol. Life Sci.* **57,** 1894–1908
20. Uversky, V. N., and Eliezer, D. (2009) Biophysics of Parkinson disease. Structure and aggregation of α-synuclein. *Curr. Protein Pept. Sci.* **10,** 483–499
21. Ringrose, J. H., van Solinge, W. W., Mohammed, S., O'Flaherty, M. C., van Wijk, R., Heck, A. J., and Slijper, M. (2008) Highly efficient depletion strategy for the two most abundant erythrocyte-soluble proteins improves proteome coverage dramatically. *J. Proteome Res.* **7,** 3060–3063
22. Han, V., Serrano, K., and Devine, D. V. (2010) A comparative study of common techniques used to measure hemolysis in stored red cell concentrates. *Vox Sang.* **98,** 116–123
23. Eliezer, D., Kutluay, E., Bussell, R., Jr., and Browne, G. (2001) Conformational properties of α-synuclein in its free and lipid-associated states. *J. Mol. Biol.* **307,** 1061–1073
24. Delaglio, F., Grzesiek, S., Vuister, G. W., Zhu, G., Pfeifer, J., and Bax, A. (1995) NMRPipe. A multidimensional spectral processing system based on UNIX pipes. *J Biomol NMR* **6,** 277–293
25. Johnson, B. A., and Blevins, R. A. (1994) NMR View. A Computer Program for the Visualization and Analysis of NMR Data. J. *Biomol. NMR* **4,** 603–614
26. Wishart, D. S., Bigam, C. G., Yao, J., Abildgaard, F., Dyson, H. J., Oldfield, E., Markley, J. L., and Sykes, B. D. (1995) ^{1}H, ^{13}C, and ^{15}N chemical shift referencing in biomolecular NMR. *J. Biomol. NMR* **6,** 135–140

27. Tinsley, R. B., Kotschet, K., Modesto, D., Ng, H., Wang, Y., Nagley, P., Shaw, G., and Horne, M. K. (2010) Sensitive and specific detection of α-synuclein in human plasma. *J. Neurosci. Res.* **88,** 2693–2700
28. Perrin, R. J., Payton, J. E., Barnett, D. H., Wraight, C. L., Woods, W. S., Ye, L., and George, J. M. (2003) Epitope mapping and specificity of the anti-α-synuclein monoclonal antibody Syn-1 in mouse brain and cultured cell lines. *Neurosci. Lett.* **349,** 133–135
29. Mbefo, M. K., Paleologou, K. E., Boucharaba, A., Oueslati, A., Schell, H., Fournier, M., Olschewski, D., Yin, G., Zweckstetter, M., Masliah, E., Kahle, P. J., Hirling, H., and Lashuel, H. A. (2010) Phosphorylation of synucleins by members of the Polo-like kinase family. *J. Biol. Chem.* **285,** 2807–2822
30. Lee, M. K., Stirling, W., Xu, Y., Xu, X., Qui, D., Mandir, A. S., Dawson, T. M., Copeland, N. G., Jenkins, N. A., and Price, D. L. (2002) Human α-synuclein-harboring familial Parkinson disease-linked Ala-53 → Thr mutation causes neurodegenerative disease with α-synuclein aggregation in transgenic mice. *Proc. Natl. Acad. Sci.* **99,** 8968–8973
31. Rockenstein, E. M., McConlogue, L., Tan, H., Power, M., Masliah, E., and Mucke, L. (1995) Levels and alternative splicing of amyloid β protein precursor (APP) transcripts in brains of APP transgenic mice and humans with Alzheimer disease. *J. Biol. Chem.* **270,** 28257–28267
32. Dusonchet, J., Bensadoun, J. C., Schneider, B. L., and Aebischer, P. (2009) Targeted overexpression of the parkin substrate Pael-R in the nigrostriatal system of adult rats to model Parkinson disease. *Neurobiol Dis* **35,** 32–41
33. Lennox, G., Lowe, J., Landon, M., Byrne, E. J., Mayer, R. J., and Godwin-Austen, R. B. (1989) Diffuse Lewy body disease. Correlative neuropathology using anti-ubiquitin immunocytochemistry. *J. Neurol. Neurosurg. Psychiatry* **52,** 1236–1247
34. Pham, E., Crews, L., Ubhi, K., Hansen, L., Adame, A., Cartier, A., Salmon, D., Galasko, D., Michael, S., Savas, J. N., Yates, J. R., Glabe, C., and Masliah, E. (2010) Progressive accumulation of amyloid-α oligomers in Alzheimer disease and in amyloid precursor protein transgenic mice is accompanied by selective alterations in synaptic scaffold proteins. *FEBS J.* **277,** 3051–3067
35. Anderson, J. P., Walker, D. E., Goldstein, J. M., de Laat, R., Banducci, K., Caccavello, R. J., Barbour, R., Huang, J., Kling, K., Lee, M., Diep, L., Keim, P. S., Shen, X., Chataway, T., Schlossmacher, M. G., Seubert, P., Schenk, D., Sinha, S., Gai, W. P., and Chilcote, T. J. (2006) Phosphorylation of Ser-129 is the dominant pathological modification of α-synuclein in familial and sporadic Lewy body disease. *J. Biol. Chem.* **281,** 29739–29752
36. Ohrfelt, A., Zetterberg, H., Andersson, K., Persson, R., Secic, D., Brinkmalm, G., Wallin, A., Mulugeta, E., Francis, P. T., Vanmechelen, E., Aarsland, D., Ballard, C., Blennow, K., and Westman-Brinkmalm, A. (2011) Identification of novel α-synuclein isoforms in human brain tissue by using an online nanoLC-ESI-FTICR-MS method. *Neurochem. Res.* **36,** 2029–2042
37. Uéda, K., Fukushima, H., Masliah, E., Xia, Y., Iwai, A., Yoshimoto, M., Otero, D. A., Kondo, J., Ihara, Y., and Saitoh, T. (1993) Molecular cloning of cDNA encoding an unrecognized component of amyloid in Alzheimer disease. *Proc. Natl. Acad. Sci.* **90,** 11282–11286
38. Jakes, R., Spillantini, M. G., and Goedert, M. (1994) Identification of two distinct synucleins from human brain. *FEBS Lett.* **345,** 27–32
39. Anderson, V. L., Ramlall, T. F., Rospigliosi, C. C., Webb, W. W., and Eliezer, D. (2010) Identification of a helical intermediate in trifluoroethanol-induced α-synuclein aggregation. *Proc. Natl. Acad. Sci.* **107,** 18850–18855
40. Bussell, R., Jr., and Eliezer, D. (2001) Residual structure and dynamics in Parkinson disease-associated mutants of α-synuclein. *J. Biol. Chem.* **276,** 45996–46003
41. Georgieva, E. R., Ramlall, T. F., Borbat, P. P., Freed, J. H., and Eliezer, D. (2008) Membrane-bound α-synuclein forms an extended helix. Long distance pulsed ESR measurements using vesicles, bicelles, and rod-like micelles. *J. Am. Chem. Soc.* **130,** 12856–12857
42. Georgieva, E. R., Ramlall, T. F., Borbat, P. P., Freed, J. H., and Eliezer, D. (2010) The lipid-binding domain of wild type and mutant α-synuclein. Compactness and interconversion between the broken and extended helix forms. *J. Biol. Chem.* **285,** 28261–28274
43. Paleologou, K. E., Oueslati, A., Shakked, G., Rospigliosi, C. C., Kim, H. Y., Lamberto, G. R., Fernandez, C. O., Schmid, A., Chegini, F., Gai, W. P., Chiappe, D., Moniatte, M., Schneider, B. L., Aebischer, P., Eliezer, D., Zweckstetter, M., Masliah, E., and Lashuel, H. A. (2010) Phosphorylation at Ser-87 is enhanced in synucleinopathies, inhibits α-synuclein oligomerization, and influences synuclein-membrane interactions. *J. Neurosci.* **30,** 3184–3198
44. Paleologou, K. E., Schmid, A. W., Rospigliosi, C. C., Kim, H. Y., Lamberto, G. R., Fredenburg, R. A., Lansbury, P. T., Jr., Fernandez, C. O., Eliezer, D., Zweckstetter, M., and Lashuel, H. A. (2008) Phosphorylation at Ser-129 but not the phosphomimics S129E/D inhibits the fibrillation of α-synuclein. *J. Biol. Chem.* **283,** 16895–16905
45. Rospigliosi, C. C., McClendon, S., Schmid, A. W., Ramlall, T. F., Barré, P., Lashuel, H. A., and Eliezer, D. (2009) E46K Parkinson-linked mutation enhances C-terminal to N-terminal contacts in α-synuclein. *J. Mol. Biol.* **388,** 1022–1032
46. Sung, Y. H., and Eliezer, D. (2007) Residual structure, backbone dynamics, and interactions within the synuclein family. *J. Mol. Biol.* **372,** 689–707
47. Croke, R. L., Sallum, C. O., Watson, E., Watt, E. D., and Alexandrescu, A. T. (2008) Hydrogen exchange of monomeric α-synuclein shows unfolded structure persists at physiological temperature and is independent of molecular crowding in *Escherichia coli*. *Protein Sci.* **17,** 1434–1445
48. Fernández, C. O., Hoyer, W., Zweckstetter, M., Jares-Erijman, E. A., Subramaniam, V., Griesinger, C., and Jovin, T. M. (2004) NMR of α-synuclein-polyamine complexes elucidates the mechanism and kinetics of induced aggregation. *EMBO J.* **23,** 2039–2046
49. Li, C., Lutz, E. A., Slade, K. M., Ruf, R. A., Wang, G. F., and Pielak, G. J. (2009) ^{19}F NMR studies of α-synuclein conformation and fibrillation. *Biochemistry* **48,** 8578–8584
50. McNulty, B. C., Tripathy, A., Young, G. B., Charlton, L. M., Orans, J., and Pielak, G. J. (2006) Temperature-induced reversible conformational change in the first 100 residues of α-synuclein. *Protein Sci.* **15,** 602–608
51. Rasia, R. M., Bertoncini, C. W., Marsh, D., Hoyer, W., Cherny, D., Zweckstetter, M., Griesinger, C., Jovin, T. M., and Fernández, C. O. (2005) Structural characterization of copper(II) binding to α-synuclein. Insights into the bioinorganic chemistry of Parkinson disease. *Proc. Natl. Acad. Sci.* **102,** 4294–4299
52. Segers-Nolten, I. M., Wilhelmus, M. M., Veldhuis, G., van Rooijen, B. D., Drukarch, B., and Subramaniam, V. (2008) Tissue transglutaminase modulates α-synuclein oligomerization. *Protein Sci.* **17,** 1395–1402
53. Wu, K. P., Weinstock, D. S., Narayanan, C., Levy, R. M., and Baum, J. (2009) Structural reorganization of α-synuclein at low pH observed by NMR and REMD simulations. *J. Mol. Biol.* **391,** 784–796
54. Azeredo da Silveira, S., Schneider, B. L., Cifuentes-Diaz, C., Sage, D., Abbas-Terki, T., Iwatsubo, T., Unser, M., and Aebischer, P. (2009) Phosphorylation does not prompt, nor prevent, the formation of α-synuclein toxic species in a rat model of Parkinson disease. *Hum. Mol. Genet.* **18,** 872–887
55. El-Agnaf, O. M., Salem, S. A., Paleologou, K. E., Curran, M. D., Gibson, M. J., Court, J. A., Schlossmacher, M. G., and Allsop, D. (2006) Detection of oligomeric forms of α-synuclein protein in human plasma as a potential biomarker for Parkinson's disease. *FASEB J.* **20,** 419–425
56. Lee, D., Lee, E. K., Lee, J. H., Chang, C. S., and Paik, S. R. (2001) Self-oligomerization and protein aggregation of α-synuclein in the presence of Coomassie Brilliant Blue. *Eur. J. Biochem.* **268,** 295–301
57. Paik, S. R., Shin, H. J., Lee, J. H., Chang, C. S., and Kim, J. (1999) Copper(II)-induced self-oligomerization of α-synuclein. *Biochem. J.* **340**, 821–828
58. Cole, N. B., Murphy, D. D., Grider, T., Rueter, S., Brasaemle, D., and Nussbaum, R. L. (2002) Lipid droplet binding and oligomerization properties of the Parkinson disease protein α-synuclein. *J. Biol. Chem.* **277,** 6344–6352
59. Shaikh, S., and Nicholson, L. F. (2008) Advanced glycation end products induce *in vitro* cross-linking of α-synuclein and accelerate the process of intracellular inclusion body formation. *J. Neurosci. Res.* **86,** 2071–2082
60. Walker, J. M. (2002) *The Protein Protocols Handbook 200*, Part II, pp. 57–60, Humana Press, Totowa, NJ
61. Selkoe, D., Choi, J., Kim, N., and Bartels, T. (2011) Nondenaturing purification of α-synuclein from erythrocytes. *Protocol Exchange*
62. Smith, D. B., and Johnson, K. S. (1988) Single-step purification of polypeptides expressed in *Escherichia coli* as fusions with glutathione *S*-transferase. *Gene* **67,** 31–40

63. Lim, K., Ho, J. X., Keeling, K., Gilliland, G. L., Ji, X., Rüker, F., and Carter, D. C. (1994) Three-dimensional structure of *Schistosoma japonicum* glutathione *S*-transferase fused with a six-amino acid conserved neutralizing epitope of gp41 from HIV. *Protein Sci.* **3,** 2233–2244
64. Parker, M. W., Lo Bello, M., and Federici, G. (1990) Crystallization of glutathione *S*-transferase from human placenta. *J. Mol. Biol.* **213,** 221–222
65. Ji, X., Zhang, P., Armstrong, R. N., and Gilliland, G. L. (1992) The three-dimensional structure of a glutathione *S*-transferase from the mu gene class. Structural analysis of the binary complex of isoenzyme 3–3 and glutathione at 2.2-Å resolution. *Biochemistry* **31,** 10169–10184
66. Ferguson, K. A. (1964) Starch gel electrophoresis. Application to the classification of pituitary proteins and polypeptides. *Metabolism* **13,** 985–1002
67. Wu, K. P., Kim, S., Fela, D. A., and Baum, J. (2008) Characterization of conformational and dynamic properties of natively unfolded human and mouse α-synuclein ensembles by NMR. Implication for aggregation. *J. Mol. Biol.* **378,** 1104–1115
68. Marsh, J. A., Singh, V. K., Jia, Z., and Forman-Kay, J. D. (2006) Sensitivity of secondary structure propensities to sequence differences between α- and γ-synuclein. Implications for fibrillation. *Protein Sci.* **15,** 2795–2804
69. Bertoncini, C. W., Fernandez, C. O., Griesinger, C., Jovin, T. M., and Zweckstetter, M. (2005) Familial mutants of α-synuclein with increased neurotoxicity have a destabilized conformation. *J. Biol. Chem.* **280,** 30649–30652
70. Kang, J. H., and Kim, K. S. (2003) Enhanced oligomerization of the α-synuclein mutant by the Cu,Zn-superoxide dismutase and hydrogen peroxide system. *Mol. Cells* **15,** 87–93
71. Krishnan, S., Chi, E. Y., Wood, S. J., Kendrick, B. S., Li, C., Garzon-Rodriguez, W., Wypych, J., Randolph, T. W., Narhi, L. O., Biere, A. L., Citron, M., and Carpenter, J. F. (2003) Oxidative dimer formation is the critical rate-limiting step for Parkinson disease α-synuclein fibrillogenesis. *Biochemistry* **42,** 829–837
72. Dedmon, M. M., Lindorff-Larsen, K., Christodoulou, J., Vendruscolo, M., and Dobson, C. M. (2005) Mapping long range interactions in α-synuclein using spin-label NMR and ensemble molecular dynamics simulations. *J. Am. Chem. Soc.* **127,** 476–477
73. Oueslati, A., Paleologou, K. E., Schneider, B. L., Aebischer, P., and Lashuel, H. A. (2012) Mimicking phosphorylation at serine 87 inhibits the aggregation of human α-synuclein and protects against its toxicity in a rat model of Parkinson disease. *J. Neurosci.* **32,** 1536–1544